

Vivianite as an important iron phosphate precipitate in sewage treatment plants

Wilfert, P.; Mandalidis, A.; Dugulan, A. I.; Goubitz, K.; Korving, L.; Temmink, H.; Witkamp, G. J.; Van Loosdrecht, M. C. M.

DOI

[10.1016/j.watres.2016.08.032](https://doi.org/10.1016/j.watres.2016.08.032)

Publication date

2016

Document Version

Accepted author manuscript

Published in

Water Research

Citation (APA)

Wilfert, P., Mandalidis, A., Dugulan, A. I., Goubitz, K., Korving, L., Temmink, H., Witkamp, G. J., & Van Loosdrecht, M. C. M. (2016). Vivianite as an important iron phosphate precipitate in sewage treatment plants. *Water Research*, 104, 449-460. <https://doi.org/10.1016/j.watres.2016.08.032>

Important note

To cite this publication, please use the final published version (if applicable).
Please check the document version above.

Copyright

Other than for strictly personal use, it is not permitted to download, forward or distribute the text or part of it, without the consent of the author(s) and/or copyright holder(s), unless the work is under an open content license such as Creative Commons.

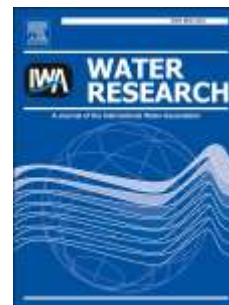
Takedown policy

Please contact us and provide details if you believe this document breaches copyrights.
We will remove access to the work immediately and investigate your claim.

Accepted Manuscript

Vivianite as an important iron phosphate precipitate in sewage treatment plants

P. Wilfert, A. Mandalidis, A.I. Dugulan, K. Goubitz, L. Korving, H. Temmink, G.J. Witkamp, M.C.M. Van Loosdrecht



PII: S0043-1354(16)30632-7

DOI: [10.1016/j.watres.2016.08.032](https://doi.org/10.1016/j.watres.2016.08.032)

Reference: WR 12303

To appear in: *Water Research*

Received Date: 23 May 2016

Revised Date: 8 August 2016

Accepted Date: 18 August 2016

Please cite this article as: Wilfert, P., Mandalidis, A., Dugulan, A.I., Goubitz, K., Korving, L., Temmink, H., Witkamp, G.J., Van Loosdrecht, M.C.M., Vivianite as an important iron phosphate precipitate in sewage treatment plants, *Water Research* (2016), doi: 10.1016/j.watres.2016.08.032.

This is a PDF file of an unedited manuscript that has been accepted for publication. As a service to our customers we are providing this early version of the manuscript. The manuscript will undergo copyediting, typesetting, and review of the resulting proof before it is published in its final form. Please note that during the production process errors may be discovered which could affect the content, and all legal disclaimers that apply to the journal pertain.

Vivianite as an important iron phosphate precipitate in sewage treatment plants

P. Wilfert^{a,b}, A. Mandalidis^a, A.I. Dugulan^c, K. Goubitz^c, L. Korving^{a,*}, H. Temmink^{a,d}, G.J. Witkamp^b and M.C.M Van Loosdrecht^b

^aWetsus, European Centre Of Excellence for Sustainable Water Technology, Oostergoweg 7, 8911 MA, Leeuwarden, The Netherlands

^bDept. Biotechnology, Delft Univ Technol, Van der Maasweg 9, 2629 HZ Delft, The Netherlands

^cFundamental Aspects Mat & Energy Grp, Delft Univ Technol, Mekelweg 15, 2629 JB Delft, The Netherlands

^dSub-department of Environmental Technology, Wageningen University, P.O. Box 8129, 6700 EV Wageningen, The Netherlands

*Corresponding author: Phone: +31-58-2843160; e-mail: Leon.Korving@Wetsus.nl

Abbreviations

CPR – Chemical Phosphorus Removal

COD – Chemical Oxygen Demand

DO - Dissolved Oxygen

DOC - Dissolved Organic Carbon

EBPR – Enhanced Biological Phosphorus Removal

Fe₂O₃ – Hematite

FeP - Iron Phosphorus Compounds

FeS_x - Iron Sulphide Compounds

IRB - Iron Reducing Bacteria

o-P - Orthophosphate

SRT – Solid Retention Time

STP – Sewage Treatment Plant

TS - Total Solids

Abstract

Iron is an important element for modern sewage treatment, inter alia to remove phosphorus from sewage. However, phosphorus recovery from iron phosphorus containing sewage sludge, without incineration, is not yet economical. We believe, increasing the knowledge about iron-phosphorus speciation in sewage sludge can help to identify new routes for phosphorus recovery. Surplus and digested sludge of two sewage treatment plants was investigated. The plants relied either solely on iron based phosphorus removal or on biological phosphorus removal supported by iron dosing. Mössbauer spectroscopy showed that vivianite and pyrite were the dominating iron compounds in the surplus and anaerobically digested sludge solids in both plants. Mössbauer spectroscopy and XRD suggested that vivianite bound phosphorus made up between 10 and 30 % (in the plant relying mainly on biological removal) and between 40 and 50 % of total phosphorus (in the plant that relies on iron based phosphorus removal). Furthermore, Mössbauer spectroscopy indicated that none of the samples contained a significant amount of Fe(III), even though aerated treatment stages existed and although besides Fe(II) also Fe(III) was dosed. We hypothesize that chemical/microbial Fe(III) reduction in the treatment lines is relatively quick and triggers vivianite formation. Once formed, vivianite may endure oxygenated treatment zones due to slow oxidation kinetics and due to oxygen diffusion limitations into sludge flocs. These results indicate

that vivianite is the major iron phosphorus compound in sewage treatment plants with moderate iron dosing. We hypothesize that vivianite is dominating in most plants where iron is dosed for phosphorus removal which could offer new routes for phosphorus recovery.

Keywords:

Iron, Phosphorus, Sewage, Sewage sludge, Mössbauer spectroscopy, Vivianite

1 Introduction

Phosphorus (P) is an essential element for all life. It is often a limiting nutrient for crops and thus a crucial part of fertilizers. Currently, the use of P is not sustainable and its supply is not guaranteed in the future: (I) Phosphate rock reservoirs, the main source of P for fertilizers, are depleting (Scholz and Wellmer, 2016; Walan et al., 2014), (II) these reservoirs are located in a few countries (De Ridder et al., 2012), (III) for current P applications and depletions regional imbalances exist (Macdonald et al., 2011; van Dijk et al., 2016) and (IV) P surpluses cause eutrophication in surface waters (Carpenter, 2008). The recovery of P from secondary resources would help to make its use in our society circular and more sustainable (Carpenter and Bennett, 2011; Childers et al., 2011).

Sewage is an important secondary source for P (van Dijk et al., 2016). In sewage treatment plants (STPs), P is typically removed to diminish eutrophication in surface waters by chemical P removal (CPR) or enhanced biological P removal (EPBR). In both cases, P is concentrated in the sewage sludge. Iron (Fe) dosing for CPR is efficient, simple and cheap (Geraarts et al., 2007; Paul et al., 2001; WEF, 2011). Future energy producing STPs rely on chemical P and chemical oxygen demand (COD) removal (Böhnke, 1977; Wilfert et al., 2015). Additionally, Fe is commonly

applied in modern sewage treatment also for other reasons than CPR. Ferric, Fe(III) and ferrous, Fe(II) iron salts are dosed as flocculants to remove COD (Li, 2005), to prevent the emission of hydrogen sulphide (H_2S) in sewer systems and digesters (Hvitved-Jacobsen et al., 2013; Nielsen et al., 2005) and to improve sludge dewatering (Higgins and Murthy, 2006). Additionally, Fe may originate from groundwater intrusion into the sewer systems (Hvitved-Jacobsen et al., 2013; Kracht et al., 2007). Thus, in most STPs, part of the P will be bound to Fe. An economic feasible recovery of P from sewage sludge containing iron phosphorus compounds (FeP), without sludge incineration, is a technological challenge that remains unsolved, also due to scarce information on FeP mineralogy in STPs (Wilfert et al 2015).

The initial reactions, after Fe(III) or Fe(II) addition to sewage and the subsequent removal of P are complex (El Samrani et al., 2004; Luedecke et al., 1989; Smith et al., 2008; Takács et al., 2006). These reactions are important as they drive primary P removal from sewage by bringing P from the liquid to the solid phase. In STPs, the solid retention time (SRT) can be a few hours, as in the A-stage of AB-processes (Böhnke, 1977; Böhnke et al., 1997), but it is usually on the time scale of 5-20 days when the conventional activated sludge process is applied (Tchobanoglous et al., 2013). In those processes, alternating redox conditions are applied to achieve COD and nitrogen removal. Hence, once formed the initial FeP may change due to oxidation of Fe(II) or reduction of Fe(III) respectively (Nielsen, 1996; Nielsen et al., 2005; Nielsen and Nielsen, 1998; Rasmussen and Nielsen, 1996) or due to aging effects (Recht and Ghassemi, 1970; Szabó et al., 2008). Most likely, the FeP, that end up in the surplus sludge and that determine the P removal efficiency of STPs, differ from the initial precipitates.

Several researchers reported the ferrous iron phosphate mineral vivianite ($\text{Fe(II)}_3[\text{PO}_4]_2 \cdot 8\text{H}_2\text{O}$) in surplus sludge and anaerobically digested sludge (Frossard et al., 1997; Ghassemi and Recht,

1971; Seitz et al., 1973; Singer, 1972). Frossard et al., 1997 were able to quantify vivianite in sewage sludge using Mössbauer spectroscopy even though the sludge samples in this study were exposed to air. This could have resulted in full/partial oxidation of Fe(II) compounds and partial transformation of vivianite to amorphous FeP (Roldan et al., 2002) or to other changes of the P fractions (Kraal et al., 2009). Additionally, all Mössbauer measurements were done at room temperature (300 K). Complex samples should ideally be measured at lower temperatures (e.g. 4.2 K) as well, to reveal unambiguously the spectral contributions and magnetic properties of the Fe phases. (Murad and Cashion, 2004).

We have investigated two STPs, with different treatment strategies to determine the fate of Fe and FeP during treatment. The STP Leeuwarden applies EBPR, additionally respectively Fe(II) or Fe(III) are dosed in two different treatment lines. The STP Nieuwveer uses the AB technology (Böhnke et al., 1997; De Graaff et al., 2015), here Fe(II) is dosed. AB-plants in combination with cold anammox have the potential to be energy factories (Jetten et al., 1997; Siegrist et al., 2008).

The fate of Fe and FeP was evaluated by various measurements on the liquid and solid fractions of the sewage (sludge) at different locations in the treatment line. Mössbauer spectroscopy (qualitative and quantitative analyses of Fe compounds), XRD (semi-quantitative analyses of all crystalline material) and SEM-EDX (particle morphology and elemental composition) were used to characterize the solid fractions. Mass balances for P and Fe helped to identify the significance of different sources (influent, external sludge, Fe dosing) and sinks (effluent, sludge disposal) for these elements. Mössbauer spectroscopy and XRD were used to estimate P bound in vivianite and sulphide extraction was used to quantify P bound to Fe. Thereby, the P recovery potential of a technology that targets specifically on FeP was determined.

Identifying the forms of FeP in activated sludge would help to obtain thermodynamic (e.g. equilibrium concentrations) and stoichiometric (molar Fe:P ratios) information that is necessary to develop technologies to recover P from FeP. Although, in literature, some indications for vivianite formation as major P compound during sewage treatment can be found, the role of vivianite and its importance has been neglected, the reason why this study was carried out.

2 Methods & Material

2.1 STPs and sampling

In the AB plant Nieuwveer (influent: $75706 \text{ m}^3 \text{ d}^{-1}$ in 2014), Fe(II) is added in the aerated ($\approx 0.3 \text{ mg dissolved oxygen (DO) L}^{-1}$) A-stage for P and COD removal. SRTs are 15 hours in the A-stage, 16 days in the B-stage (DO in aerated sections $\approx 1.8 \text{ mg DO L}^{-1}$) and 25 days during anaerobic digestion. In the EBPR plant Leeuwarden ($38,000 \text{ m}^3 \text{ d}^{-1}$ in 2014), the influent is split in two treatment lines (60 % of the sewage goes to Line 1). Besides for CPR, Fe is dosed to prevent H_2S emissions into the biogas during anaerobic digestion. In Line 1, Fe(III) is dosed and in Line 2 Fe(II) is dosed in the nitrification zone ($\approx 1.5 \text{ mg DO L}^{-1}$). SRTs before digestion are around 15 days (50 % in the aerated zone) and during anaerobic digestion around 42 days. The digesters of both STPs, receive external sludge which accounts for about 30 % (Nieuwveer) and about 25 % (Leeuwarden) of the total digested sludge. At both locations, samples were taken to analyse the composition of the of the sewage (sludge). From these measurements (Table A. 1 and Table A. 2) Fe and P mass balances were calculated. To calculate Fe and P loads, average daily flow rates of the sampling days were used. Samples were taken between December 2014 and March 2015, after a period of 48 h without precipitation. The STP Leeuwarden was sampled three times. Results

reported in Table A. 1 and for the mass balances are average values of the triplicate measurements and of the daily loads of these samplings. The STP Nieuwveer was sampled once in March 2015.

Samples were stored and transported in cooling boxes on ice to reduce microbial activity. Sample processing started 1 h (Leeuwarden) and 3 h (Nieuwveer) after sampling. Sample drying started latest 8 h after sampling and was completed within 24 h. Sampling and sample processing were done under anaerobic conditions to prevent oxidation and degassing of samples. Sewage was collected; using syringes with attached tubing that were washed several times with sewage. Sewage sludge was taken from valves using a funnel with attached tubing. Samples were then filled in serum bottles. To rinse bottles, about three times their volume was flowed through the bottle by inserting the end of the tubing to the bottom of the bottle. Then the bottles were sealed with butyl rubber stoppers (referred to as anaerobic samples hereafter). With these samples the composition of the liquid phase was determined and material for solid analyses was obtained. For total solids (TS), volatile solids (VS) and to determine the total elemental composition of the sewage (sludge), separate samples, without special pre-cautions to prevent sample oxidation, were taken (hereafter, referred to as mass balance (MB) samples). Separate sampling was considered to be necessary as the TS content of the anaerobic samples could change due to rinsing of serum bottles.

In Nieuwveer, the influent sample was a mixture of raw influent and recirculated effluent (40 % of the effluent is recirculated). For the mass balances, the Fe and P concentrations of the raw effluent were calculated. The external sludge sample was taken from a pre-storage tank, and contained an unknown mixture of external sludge. In Leeuwarden, P loads from external sludge were below the detection limit and had to be calculated from the difference in P loads before and after digestion.

2.2 Analyses

Oxidation-Reduction Potential (ORP), pH and conductivity were measured potentiometrically in the plants. Total elemental composition of MB samples were determined after microwave assisted acid digestion ($\text{HNO}_3=69\%$, 15 min, 180°C) followed by ICP-OES. Total solids and VS were measured according to standard methods (APHA, AWWA, WEF, 1998). For total alkalinity measurements, 10 mL MB sample was titrated to $\text{pH}=4.5$ with 0.1 N HCl (APHA, AWWA, WEF, 1998).

The anaerobic samples were transferred into plastic centrifuge tubes inside an anaerobic glovebox (95 % $\text{N}_2/5\%$ H_2 , $\text{O}_2<10$ ppm) and centrifuged (15 min, 3200 G). Dissolved elemental compositions (ICP-OES), dissolved anions (IC) and dissolved organic carbon, DOC (LC-OCD) were determined after filtration of the supernatant ($0.45\ \mu\text{m}$) inside the glovebox. Dissolved Fe(II)/Fe(III) was determined in the filtrate using the ferrozine method according to Viollier et al., 2000. In short, an appropriate sample volume was added to 100 μL ferrozine reagent and made up to a total volume of 1100 μL using Milli-Q water. After 15 minutes the absorbance of the ferrozine-Fe(II) complex was recorded. Subsequently, to reduce all Fe(III) to Fe(II), 150 μL of a $1.4\ \text{mol L}^{-1}$ hydroxylamine solution was added to 800 μL of this solution. The reduction time was 12 h (30°C) to make sure that organic complexed Fe(III) was completely reduced (Rasmussen and Nielsen, 1996; Verschoor and Molot, 2013). Eventually, 50 μL of an $10\ \text{mol L}^{-1}$ ammonium acetate buffer solution was added and the absorbance was again measured. With these information the Fe(II) and Fe(III) concentration can be calculated. All ferrozine measurements were confirmed by measuring total Fe by ICP-OES. Additionally, Fe(II)/Fe(III) stock solutions were added to filtrates to test the reliability of the photometric measurements (Table 1). For sulphide (S^{2-})

measurements, samples were filtered inside the glovebox into a zinc acetate solution (0.8 M), stored in the dark and measured after 24 h by the methylene blue method (Cline, 1969).

Solid material was derived from centrifuge pellets of the anaerobic samples. Inside the glovebox, pellets were finely spread on glass plates, dried (25 °C, 24 h, in the dark) and grinded using a mortar and pestle. Vivianite can be found when samples are dried at room temperature, even in the presence of oxygen. Higher temperatures for sample drying should be avoided. Above 70 °C, in the presence oxygen, vivianite is transformed within hours into an amorphous iron phosphate compound (Čermáková et al., 2015). Thus, in such sludge samples, vivianite disappears (Poffet, 2007).

Samples for XRD analyses were filled in glass capillaries and sealed first with modelling clay and then superglue. Right before analyses, glass capillaries were sealed using a burner. The measurements were done on a PANalytical X'Pert PRO diffractometer with Cu-K α radiation (5-80 °2 θ , step size 0.008°). The results from XRD analyses were made semi-quantitative by determining the amorphous and crystalline peak area of the spectra (Origin Pro 9). This allows the determination of the degree of crystallinity and thus of the total mineral share of the sample. All samples that were analysed by Mössbauer spectroscopy were also analysed by XRD. In addition, two samples that were sampled in the aerated treatment lines (referred to as A-stage and Line 2 activated sludge samples) were analysed using XRD.

For Mössbauer analyses, samples were filled in plastic rings, sealed with Kapton tape and super glue and then wrapped in parafilm. It was expected that considerable amounts of P are bound in vivianite, thus a vivianite standard was prepared according to Roldan et al., 2002. Transmission ⁵⁷Fe Mössbauer spectra were collected at 4.2 and 300 K with conventional constant-acceleration

and sinusoidal velocity spectrometers using a $^{57}\text{Co}(\text{Rh})$ source. Velocity calibration was carried out using an $\alpha\text{-Fe}$ foil. The Mössbauer spectra were fitted using Mosswin 4.0 (Klencsár, 1997). Morphology and elemental compositions of sludge particles in the grinded solids was also analysed by SEM-EDX. Samples for SEM-EDX were exposed to air during measurements.

Extractability of Fe in digested sludge was investigated using water, to extract water soluble Fe (pH=7, Wolf et al., 2009). Na-pyrophosphate solution (0.1 mol L^{-1} , pH=9.5) was used to extract and quantify organic bound Fe. Pyrophosphate was used to extract organic bound Fe and Fe minerals mainly in soil but also from sewage sludge, vivianite was partially dissolved with this extract (Carliell-Marquet et al., 2009; McKeague, 1967; van Hullebusch et al., 2005). With pyrophosphate extraction no distinction between Fe(II)/Fe(III) could be made. Ammonium oxalate (0.2 mol L^{-1} $\text{NH}_4\text{-oxalate}$, pH=3) extracts poorly crystalline Fe, it was used to determine Fe(II)/Fe(III) in activated sludge before (Rasmussen and Nielsen, 1996). Each extraction was done in separate butyl rubber stoppered serum bottles, the extracts were added to wet sludge (n=3). Oxygen in the extracts was removed using headspace gas exchange equipment with a gas mixture containing 70 % N_2 and 30 % CO_2 in 5 cycles. The extract:TS ratios were 100:1 for H_2O and pyrophosphate and 1000:1 for oxalate. All samples were shaken in the dark (16 h, 30 °C, 100 rpm) before analysing Fe in the filtered ($0.45 \mu\text{m}$) but not centrifuged extracts.

2.3 Estimate P bound to Fe

P bound in vivianite was calculated from results of semi-quantitative XRD and Mössbauer spectroscopy. Additionally, to determine sulphide extractable P, 0.5 molar Na_2S solution was added to 2 L digested sludge (molar Fe:P=0.55) and surplus sludge from Line 1 (molar Fe:P=0.25) from Leeuwarden and to digested sludge from Nieuwveer (molar Fe:P =0.73) in molar ratios $\text{S}^{2-}:\text{Fe}$ of 1.5. These samples were taken several months before/after the other samples. For

Leeuwarden, molar Fe:P were very similar to the sludge used for other analyses, digested sludge showed an Fe:P=0.56 and Line 1 an Fe:P=0.28 but for Nieuwveer the sludge for the sulphide experiments had a lower Fe:P (0.73 vs 0.89). It was assumed that sulphide extracts specifically P bound to FeP (Kato et al., 2006). The experiments were done in a gastight reactor with pH control (pH=7.5) with a reaction time of at least 24 h. Samples from the reactor were taken using N₂ flushed syringes, filled in N₂ rinsed plastic centrifuge tubes under a stream of N₂ and centrifuged (15 min, 3200 G). Subsequently, sulphide, ortho-P (o-P) and the elemental composition were determined in samples that were filtered using N₂ flushed syringes and filters (0.45 µm). At the end of these experiments at least 1 mmol sulphide L⁻¹ was still in solution indicating that the extraction was not sulphide limited. The maximum amounts of P that could be bound to Fe, Mg and Al were quantified by using the elemental composition of the TS (Table A. 1 & Table A. 2). For these calculations it was assumed that all solid Mg is present as struvite (molar Mg:P =1), all Fe as vivianite (molar Fe:P=1.5) and Al as a precipitate with a molar Al:P of 1.5 (Hsu, 1976).

3 Results

3.1 Mass balances

In the STP Leeuwarden, mass balances showed, that the influent Fe load equals approximately the dosed Fe (Figure 1A). The effluent load was approximately 15 % of the influent Fe and 10 % of the influent P. The solid molar Fe:P ratio almost doubles from 0.33 before to 0.57 after anaerobic digestion due to digestion of external sludge with a high Fe (8.4 g Fe /kg sludge) and low P (not detectable) content. About 95 % of the external sludge originates from two cheese factories which use Fe(III) as flocculent.

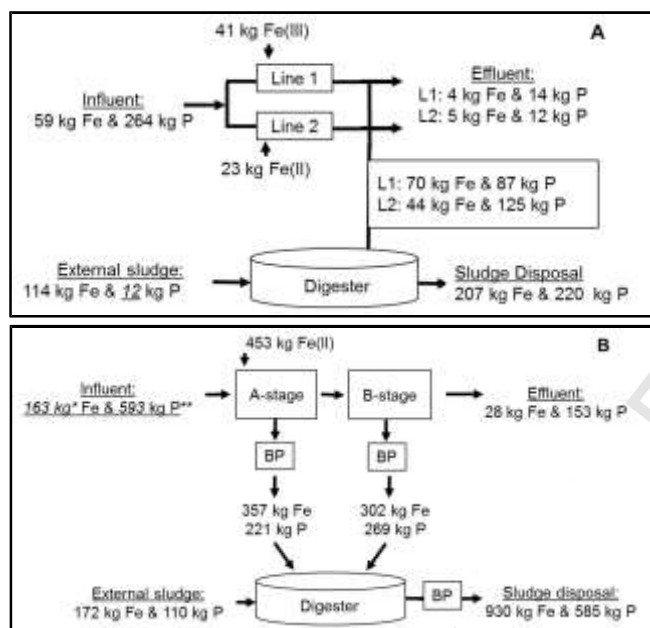


Figure 1: Daily mass balances for Fe and P in the STPs Leeuwarden (A) and Nieuwveer (B). Underlined numbers were calculated (BP = belt press).

For Nieuwveer, the mass balance showed that, dosed Fe is about three times the Fe entering via the influent (Figure 1B). The effluent load was 15 % of the influent Fe and 25 % of the influent P. The Fe and P loads from the A and B stage to the anaerobic digestion are similar. During digestion, the molar Fe:P ratio increased, due to external sludge, from 0.76 to 0.89.

The mass balances were established by a single sampling campaign in Nieuwveer and three sampling campaigns in Leeuwarden. It was not intended to make a comprehensive mass balance which would require several samplings throughout the year. The mass balance served to identify main Fe sources and sinks in the STPs. For Nieuwveer, the calculated P loads of the influent, effluent and into the digester were about 20 % higher, the external sludge P input about 20 % lower when compared to the average yearly P loads for 2014 which were determined from daily P measurements on pooled samples (number from yearly balance/from our balance): influent (460 vs 593 kg P d⁻¹), effluent (118 vs 153 kg P d⁻¹), external sludge (139 vs 110 kg P d⁻¹) and to the digester (411 vs 490 kg P d⁻¹). Since loads (except for the external sludge) were consistently

higher for our measurements it can be assumed that patterns of Fe and P loads represent typical situations for the STP. For Leeuwarden, average yearly P loads in 2014 in the influent were also about 20 % higher (318 vs 264 kg P d⁻¹) and almost the same for the effluent (28 vs 26 kg P d⁻¹). Phosphorus flows into the digester are not regularly determined in Leeuwarden.

The maximum gap for the mass balance was about 15 % for Fe in the STP Nieuwveer, mainly caused by an excess of Fe leaving the digester. In contrast, the gap in the P mass balance was only 5 %. The gap in the Fe balance is most likely due to the lack of a representative external sludge sample. In Nieuwveer, external sludge is delivered in irregular intervals from various STPs applying CPR (Al/Fe dosing) and EBPR respectively. The external sludge sample in Nieuwveer was taken from a storage tank that, most likely, contained sludge also from a non Fe dosing plant. This explained why we underestimate Fe input into the digester whereas the P loads can be traced back.

3.2 Dissolved Fe(II)&Fe(III)

Fe(II)/Fe(III) stock solutions were added (n=3) to filtrates, obtained from digested sludge and from surplus sludge of Line 1 in Leeuwarden, to test the reliability of the ferrozine method (Table 1). In filtrates from surplus sludge, Fe(II) was overestimated by about 7 % and Fe(III) by about 4 %. In filtrates from digested sludge Fe(II) was added. Here, Fe(II) was underestimated by 2 % and Fe(III) overestimated by about 5 %. When Fe(III) was added it was overestimated by about 1 %. These results indicate that the method can reliably detect dissolved Fe(II) and Fe(III) in sewage samples.

After digestion, dissolved Fe in Leeuwarden sludge was surprisingly dominated by Fe(III), 1.6 mg L⁻¹ (Table 1). Also in digested sludge in Nieuwveer about half of the dissolved Fe was detected as

Fe(III), 3.0 mg L⁻¹. In general, dissolved Fe in most samples was dominated by Fe(III). This Fe(III) could be free Fe(III) or Fe(III) which was complexed by organic ligands such as humic substances (Table 1, Buffle, 1990).

Although standard addition was successful, the results should, especially after digestion, be regarded with some caution. Fe(II)/Fe(III) were determined reliably, even in the presence of dissolved organic matter (DOM, 16–25 mg DOC L⁻¹) using the ferrozine method (Verschoor and Molot, 2013; Viollier et al., 2000). However, Viollier et al., 2000, added Fe(III) only. Verschoor and Molot, 2013 found Fe(II) and Fe(III) successfully back. Yet, when added, Fe(II) could be present as free Fe(II), whereas the Fe(II) that was already in the sample could partly also be present in complexed forms (Buffle, 1990). In surplus sludge, dissolved organic matter was on the same order of magnitude (Nieuwveer A-stage: 15 mg DOC L⁻¹, Leeuwarden Line 1: 20 mg DOC L⁻¹) compared to the successful standard additions described before. In digested sludge, DOC concentrations were much higher, in Nieuwveer, 320 mg DOC L⁻¹ and in Leeuwarden, 126 mg DOC L⁻¹.

With the ferrozine assay, as we applied it, only free Fe(II) was detected (Jackson et al., 2012). When part of the Fe(II) was complexed by DOM, it was not detected in our first step, in which Fe(II) is quantified. Subsequently, to determine Fe(III), the sample pH was lowered, a reducing agent was added and the sample incubated (12 h). Under these conditions, complexed Fe(II) is mobilized and could be incorrectly assigned to Fe(III) (Gaffney et al., 2008; Jackson et al., 2012, Rasmussen and Nielsen, 1996). That also explains why total Fe levels from ICP-OES and from the ferrozine measurements matched very well. With ICP-OES free and complexed Fe is detected. To measure free and total Fe(II) in the samples the method of Gaffney et al., 2008 could be established for sewage samples. Additionally, a complementary method to determine Fe

speciation e.g. by voltammetry would help to eliminate analytical uncertainties (Buffle, 1990). In Leeuwarden, samples from Lines 1 and 2 and from the influent were on-site filtered and directly added in Ferrozine to test if free Fe(II) is present, no colour reaction was visible.

Despite all efforts, it cannot be excluded that part of the Fe(II) was oxidized during sampling or sample processing due to high sensitivity of Fe(II) to oxygen (Verschoor and Molot, 2013).

Subsequently, total dissolved Fe concentrations may decrease due to precipitation of ferric iron oxides. Ferrous iron can even get microbial oxidized in absence of oxygen (Nielsen and Nielsen, 1998). An opposing mechanism, that could occur after sampling and during sample transport, is the conversion of solid Fe(III) oxides to soluble Fe(II) by iron reducing bacteria (IRB).

Accordingly, dissolved Fe(II) concentrations doubled within 24 h in samples from the A-stage and B-stage in Nieuwveer when they were incubated at 30 °C (data not shown).

Classifying complexed Fe(II) as Fe(III) by the ferrozine assay and oxygen contamination, could explain the presence of dissolved Fe(III) after the anaerobic digestion. From a chemical point of view all dissolved Fe should be present as Fe(II). During anaerobic digestion, highly reducing conditions, including the formation of strong reducing agents like sulphide, prevail for more than three weeks. Also others found significant amounts of dissolved Fe(III) after similar periods of anaerobic incubation (Cheng et al., 2015). An increase of the oxidation-reduction potential over time could indicate that anaerobic conditions did not prevail in these experiments. In our discussion we will focus on total dissolved iron levels instead of the oxidation state of the dissolved Fe.

Table 1: Dissolved Fe(II) and Fe(III) measurements from STPs Leeuwarden and Nieuwveer

	ID	Fe(II) mg L ⁻¹	Fe(III) mg L ⁻¹	Fe (total) mg L ⁻¹
Leeuwarden	Surplus sludge Line 1, Fe(III)	0.1	0.5	0.6
	Activated sludge Line 2, Fe(II)	0.1	0.5	0.6
	Surplus sludge Line 2, Fe(II)	0.6	0.6	1.1
	Digested sludge	0.6	1.6	2.1
Nieuwveer	A-stage: after FeII dosing	0.0	0.8	0.8
	A-stage: Surplus Sludge	18.3	12.7	31.0
	B-stage: Surplus Sludge	0.0	1.9	1.9
	Digested sludge	2.9	3.0	5.9
Standard addition	Filtrate (undigested) + Fe(II): 11.8 mg L ⁻¹	12.7 (±0.24)	0	12.7
	Filtrate (undigested) + Fe(III): 11.1 mg L ⁻¹	0	11.6 (±0.0)	11.6
	Filtrate (digested) + Fe(II): 11.3 mg L ⁻¹	11.1 (±0.08)	0.6 (±0.14)	11.7
	Filtrate (digested) + Fe(III): 10 mg L ⁻¹	0	10.1 (±0.5)	10.1

3.3 Solids

3.3.1 XRD

XRD analyses revealed that vivianite and quartz were present in all samples (all XRD diffractograms and peak assignments are included in the supporting information). In the STP Leeuwarden, struvite was the dominating crystalline P phase (Table 2). During anaerobic digestion the relative share of struvite decreases compared to quartz and vivianite. In the STP Nieuwveer vivianite, as the only P containing crystalline phase, was detected in all samples. In digested solids and both A-stage samples from Nieuwveer, a peak at around 29.4 °2 θ with intensities between 3.9 and 8.6 % could not be assigned.

Table 2: Results of semi quantitative XRD and VS analyses expressed as % of the total solids.

	Sampling station	Quartz (%)	Vivianite (%)	Struvite (%)	XRD amorphous (%)	VS (%)
Leeuwarden	Line 1, Fe(III): Surplus sludge	7	2	11	80	70
	Line 2, Fe(II): Activated sludge	7	3	10	79	66
	Line 2, Fe(II): Surplus sludge	6	3	7	84	68
	Digested sludge	21	6	11	63	62
Nieuwveer	A-stage: Activated Sludge	10	7	0	83	78
	A-stage: Surplus Sludge	8	6	0	86	80
	B-stage: Surplus Sludge	11	8	0	81	78
	Digested sludge	11	8	0	63	60

3.3.2 SEM-EDX

In both STPs, no large particles with an overlap of Fe and P were found before the anaerobic digestion using SEM-EDX. Iron and P were homogenously distributed in the samples. After anaerobic digestion larger FeP particles (between 20 and 150 μm in diameter) with different crystalline morphologies were found (Figure 2). These particles showed Fe:P ratios between 1.1 and 1.7 when measured by EDX.

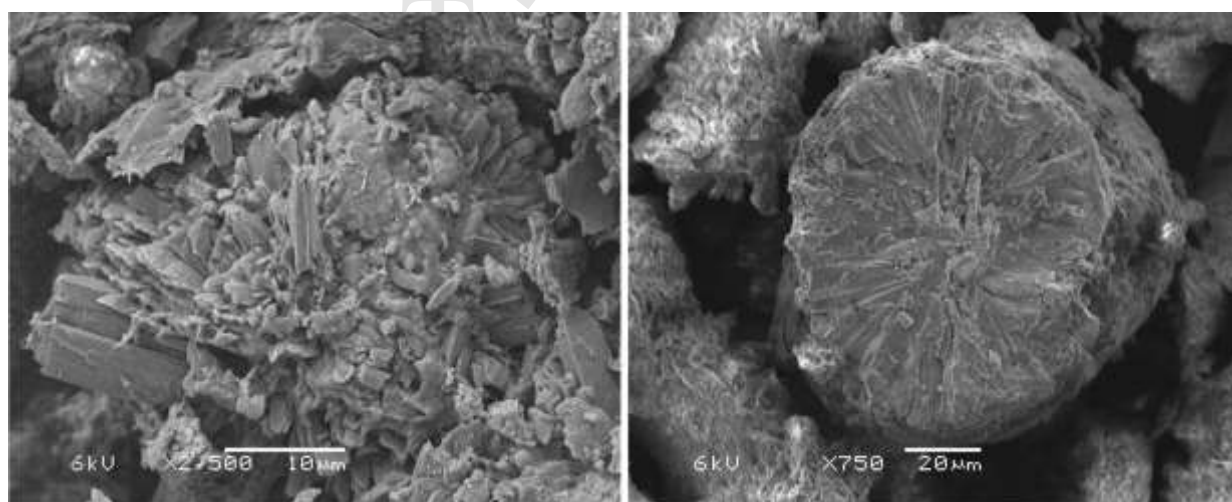


Figure 2: SEM images of particles in digested sludge solids sampled in Leeuwarden (left) and Nieuwveer (right). EDX showed Fe:P ratios between 1.1 (Leeuwarden) and 1.7 (Nieuwveer).

3.3.3 Mössbauer spectroscopy

Results of Mössbauer measurements at 4.2 K are summarized in Table 3 (all spectra and measurements at 300 K are included in the supporting information). Mössbauer spectroscopy at liquid helium temperature is more powerful as it reveals unambiguously the oxidation states and magnetic properties of the different Fe structures. The samples from Leeuwarden with digested solids and the vivianite standard showed signs of oxidation (25 to 28 % of vivianite was oxidized in the standard and in digested sludge respectively). Before measurements, these samples were sealed followed by storage at ambient atmosphere inside glass bottles with screw caps for about 1 month. Subsequently, other samples were stored inside the glovebox until measurement and no signs of oxidation were visible, as indicated by the absence of oxidized vivianite.

The spectra acquired with the vivianite standard (Figure 3) showed that about 75 % of the vivianite was not affected by oxidation and allowed to obtain a spectrum with parameters that are in good agreement with the literature for the two Fe(II) sites (Gonser and Grant, 1976). The oxidized magnetically split Fe(III) species in this standard might be an intermediate valence state between Fe(III) and Fe(II) like in magnetite (Harker and Pollard, 1993). Others suggested that oxidation of vivianite results in the formation of amorphous FeP (Miot et al., 2009), Lepidocrocite (Roldan et al., 2002) or lipscombite, beraunite or rockbridgite (Leavens, 1972).

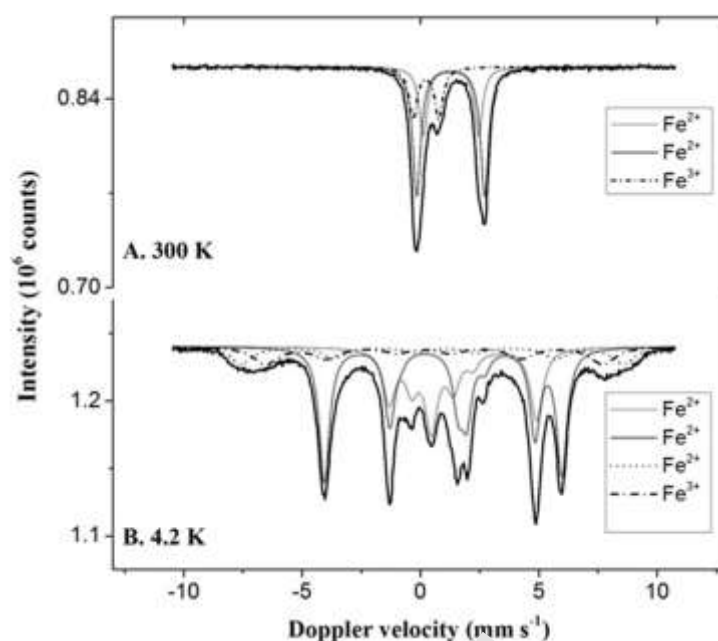


Figure 3: Mössbauer spectra obtained at different temperatures with the vivianite standard.

Samples taken from Line 1, Fe(III) dosing and Line 2, Fe(II) dosing in Leeuwarden were virtually the same. Between 94 and 96 % of the total Fe was Fe(II). Iron in vivianite represented 36 and 32 % of the total Fe in Lines 1 and 2 respectively. The significant (33 and 35 %) paramagnetic contribution to the spectra which was not magnetically split at 4.2 K was assigned to Fe(II) in pyrite, FeS₂. All other Fe species in these samples (summing up to about 30 %) could not be decisively assigned. Mössbauer spectra of a digested sludge sample taken in Leeuwarden to which sulphide was added contained the unknown Fe(II) compound that was still paramagnetic at 4.2 K (data not shown as this sample was exposed to oxygen), which contributed 20-21 % to the total Fe pool in the samples from Lines 1 and 2. Thus, we assumed this very well defined compound ($\Gamma = 0.4 \text{ mm s}^{-1}$) is a sulphur phase. However, many iron sulphide (FeS_x) and iron sulphate compounds can be excluded as they are magnetic split at 4.2 K or because they have different Mössbauer parameters (Mullet et al., 2002; Sklute et al., 2015; Yoshida and Langouche, 2013). The presence of FeP minerals cannot be excluded (Dyar et al., 2014), for instance, the Mössbauer parameters of

anapaite, $\text{Ca}_2\text{Fe}^{2+}(\text{PO}_4)_2 \cdot 4\text{H}_2\text{O}$ are close to the values we obtained (Eeckhout et al., 1999).

Overall, we cannot assign this spectra to a certain Fe phase. The Fe(III) phase is an iron oxide possibly hematite, Fe_2O_3 (Murad and Cashion, 2004).

The spectra obtained for the digested sludge sample in Leeuwarden showed that vivianite was the only FeP present (73 %). About 28 % of Fe comes from oxidized vivianite and 45 % of the Fe from vivianite unaffected by oxidation. The remaining 27 % of Fe(II) in this sample was pyrite.

In the samples from the STP Nieuwveer, Fe(II) dominated as well. The samples contained vivianite, pyrite, an Fe(III) having Mössbauer parameters resembling those of hematite, Fe_2O_3 (Murad and Cashion, 2004) and a paramagnetic (doublet) Fe(II) species that might be assigned to vivianite. The isomer shift of this Fe(II) is close to the one of vivianite, and the quadrupole splitting is also consistent with paramagnetic vivianite. Our measurements were made close to the Neel temperature (magnetic ordering temperature) of vivianite (12 K). It could be that some dispersed vivianite structures or vivianite structures with impurities are still paramagnetic at 4.2 K. The quantification of vivianite using XRD suggested that this unknown Fe(II) is vivianite (Table 4). However, this Fe(II) could also be vivianite overlapping with another phase; as well as it can be another Fe compound other than vivianite. In the surplus sludge of the A-stage about 69 % of the Fe was present as vivianite, additional 18 % as the potential vivianite phase, 9 % as pyrite and 4 % as Fe_2O_3 . The Fe in the surplus sludge sampled from the B-stage was assigned to vivianite (55 %), to the potential vivianite phase (33 %), pyrite (7 %) and to Fe_2O_3 (5 %). In digested solids, 54 % of the Fe could be firmly assigned to vivianite, 27 % were assigned to the potential vivianite phase, the share of pyrite was (15 %) and the remaining Fe (4 %) was assigned to Fe_2O_3 . For the subsequent discussions, it was assumed that the Fe(II) species that could not clearly be assigned to vivianite with Mössbauer spectroscopy was in fact vivianite.

404 In all samples from Nieuwveer and in digested sludge from Leeuwarden no iron phosphate
 405 minerals besides vivianite were present. In surplus sludge from Leeuwarden the presence of other
 406 FeP phases than vivianite, cannot be excluded. Only, minor fractions of P can be adsorbed to the
 407 Fe_2O_3 .

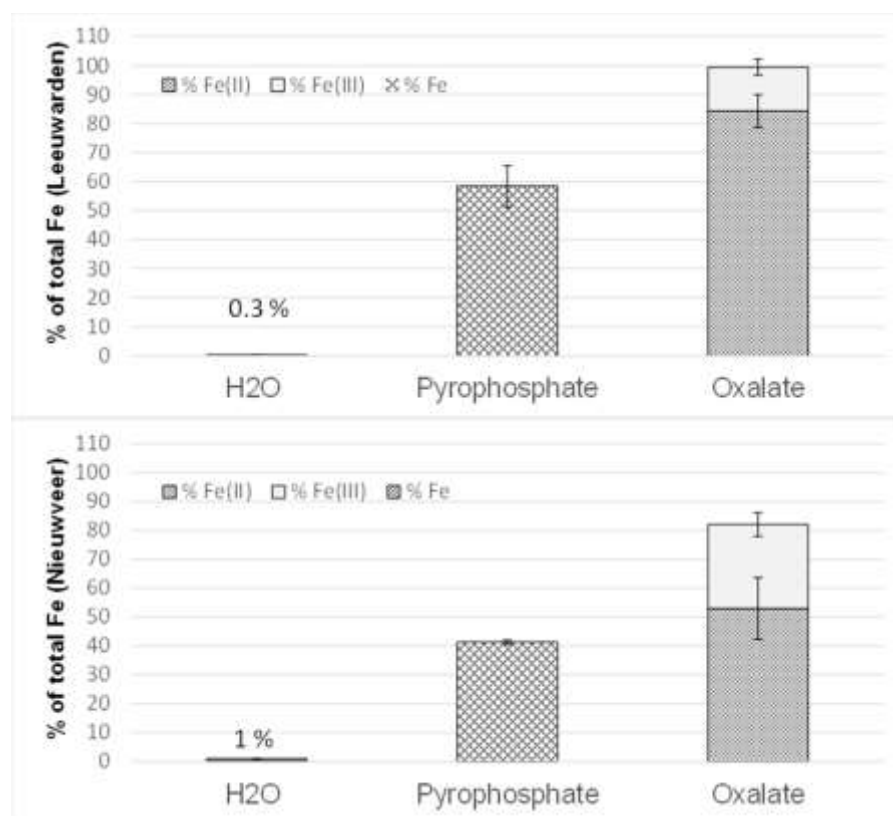
408 *Table 3: Results of Mössbauer measurements at 4.2 K. Experimental uncertainties: Isomer shift (IS): \pm*
 409 *0.01 mm s^{-1} ; Quadrupole splitting (QS): $\pm 0.01 \text{ mm s}^{-1}$; Line width (Γ): $\pm 0.01 \text{ mm s}^{-1}$; Hyperfine field: \pm*
 410 *0.1 T ; Spectral contribution: $\pm 3\%$.*

Sample	IS ($\text{mm}\cdot\text{s}^{-1}$)	QS ($\text{mm}\cdot\text{s}^{-1}$)	Hyperfine field (T)	Γ ($\text{mm}\cdot\text{s}^{-1}$)	Phase	Spectral contribution (%)
Leeuwarden Surplus Sludge Line 1: (Fe(III)) dosing	0.27	0.88	-	0.84	Fe^{2+} Pyrite	33
	0.37	0.05	51.8	0.58	Fe^{3+} Fe_2O_3	6
	0.93	-	19.3	0.74	Fe^{2+}	5
	1.29	2.47	-	0.47	Fe^{2+}	20
	1.01	1.00	11.4	1.07	Fe^{2+} Vivianite I	14
	1.26	3.71	24.8	1.07	Fe^{2+} Vivianite II	22
Leeuwarden Surplus Sludge Line 2: (Fe(II)) dosing	0.29	0.84	-	0.87	Fe^{2+} Pyrite	35
	0.37	-0.20	51.4	0.58	Fe^{3+} Fe_2O_3	4
	1.07	-	24.7	0.77	Fe^{2+}	8
	1.31	2.48	-	0.46	Fe^{2+}	21
	1.01	0.61	11.4	1.07	Fe^{2+} Vivianite I	15
	1.11	3.37	26.4	1.07	Fe^{2+} Vivianite II	17
Leeuwarden digested solids	0.42	0.79	-	0.72	Fe^{2+} Pyrite	27
	0.50	-0.84	46.0	1.41	Fe^{3+} Oxidized	15
	0.71	0.81	46.3	1.41	Fe^{2+} vivianite	13
	1.20	0.50	10.0	1.18	Fe^{2+} Vivianite I	24
	1.25	2.70	26.7	1.18	Fe^{2+} Vivianite II	21
Nieuwveer Surplus sludge A-stage	0.27	1.00	-	0.92	Fe^{2+} Pyrite	9
	0.38	-0.19	51.9	0.86	Fe^{3+} Fe_2O_3	4
	1.21	2.79	-	0.79	Fe^{2+} Dispersed vivianite	18
	1.22	2.27	15.0	0.64	Fe^{2+} Vivianite I	21
	1.21	3.13	26.4	0.64	Fe^{2+} Vivianite II	48
Nieuwveer Surplus sludge B-stage	0.33	0.88	-	0.87	Fe^{2+} Pyrite	7
	0.37	-0.14	49.8	0.86	Fe^{3+} Fe_2O_3	5
	1.16	2.92	-	0.92	Fe^{2+} Dispersed vivianite	33
	1.26	2.23	14.9	0.93	Fe^{2+} Vivianite I	18
	1.18	3.32	26.2	0.93	Fe^{2+} Vivianite II	37
Nieuwveer Digested solids	0.33	0.88	-	0.87	Fe^{2+} Pyrite	15
	0.37	0.20	48.9	0.86	Fe^{3+} Fe_2O_3	4
	1.21	2.86	-	1.23	Fe^{2+} Dispersed vivianite	27
	1.16	2.21	15.0	0.77	Fe^{2+} Vivianite I	15
	1.20	3.05	26.8	0.77	Fe^{2+} Vivianite II	39
Vivianite Standard	0.35	0.45	44.2	1.24	Fe^{3+} Oxidized	13
	0.77	-0.54	50.2	1.15	Fe^{2+} vivianite	12
	1.35	2.36	14.8	0.64	Fe^{2+} Vivianite I	29
	1.36	3.14	27.4	0.53	Fe^{2+} Vivianite II	46

411

3.3.4 Extractions

Water, pyrophosphate and ammonium oxalate were used to extract Fe from digested sludge sampled in Leeuwarden (Figure 4A) and Nieuwveer (Figure 4B). Water was the mildest extract and dissolved 0.3 and 1 % of the total solid Fe in Leeuwarden and Nieuwveer respectively. This was expected, considering the relatively low solubility of FeS_x and vivianite that dominated the digested sludge samples (Al-Borno and Tomson, 1994; Davison, 1991). However, in both STPs about 60 % of the water extractable Fe was Fe(III). During pyrophosphate extraction all dissolved Fe species were quantified, summing up to between 40 % (Nieuwveer) and 60 % (Leeuwarden) of the Fe. Considering the Mössbauer measurements, Fe bound in pyrite or vivianite must be part of this fraction. Thus, the Fe extracted using pyrophosphate was mainly of non-organic origin. Pyrophosphate extracts rather Fe from vivianite than from FeS_x (Carliell-Marquet et al., 2009). In Leeuwarden, the Fe fraction in pyrophosphate (58 ± 7 %) is in a similar range as vivianite (57 %, Mössbauer spectroscopy). However, in Nieuwveer, the pyrophosphate extracted Fe (41 ± 1 %) was much less than Fe bound in vivianite (81 %, Mössbauer spectroscopy). Ammonium oxalate extracted from Leeuwarden digested sludge all Fe (85 % as Fe(II)) and around 80 % of the Fe in Nieuwveer digested sludge (65 % as Fe(II)). Compared to the Mössbauer measurements, this indicates that the oxalate extraction and subsequent spectrophotometric determination of Fe(II)/Fe(III) overestimate the Fe(III) content by about 10 and 25 %. The described uncertainties for the spectrophotometric measurements for dissolved Fe(II)/Fe(III) could also affect the results of the Fe extraction.



432 Figure 4: Extraction of Fe from digested sludge using different extracts. The error bars indicate standard
 433 deviation (n=3).

434 3.3.5 P bound to FeP

435 The maximum amount of P bound that could be bound to Fe was estimated by using the elemental
 436 composition of the solids. Sulphide extraction was used to dissolve P bound to Fe. Phosphorus
 437 bound in vivianite was determined by semi-quantitative XRD and by Mössbauer spectroscopy
 438 (Table 4). The results for Leeuwarden indicate that in surplus sludge between 9 % (Mössbauer
 439 spectroscopy) and 13 % (XRD) and after digestion between 18 % (XRD) and 29 % (Mössbauer
 440 spectroscopy) of the P is bound in vivianite. According to XRD, the majority of P was bound in
 441 struvite in surplus (43 %) and digested sludge (35 %). These values are higher than the maximum
 442 values obtained from the elemental compositions . Thus, semi quantitative XRD overestimated the
 443 struvite content in the sludge.

In the A-stage and the B-stage, estimates were in good agreement, about 50 % of the P in the A-stage and about 40 % of the P in the B-stage were bound in vivianite. After digestion, the estimates differ considerably between sulphide extraction (31 % of P bound to Fe) and Mössbauer spectroscopy and XRD (the latter two suggested 47 % and 53 % of the P are bound in vivianite). Additional, in Nieuwveer and Leeuwarden a maximum of 25 and 8 % of the total P could be bound to Al respectively.

Table 4 indicates that, the elemental compositions of the samples tends to overestimate P bound to Fe as it does not take into account non Fe-FeP species (e.g. iron oxides, FeS_x or organic bound Fe). The same principle applies in estimating P bound to Mg in struvite or to Al in aluminium phosphorus compounds (AlP). XRD may underestimate P bound to Fe as only the P bound to vivianite is detected. Also Mössbauer spectroscopy may underestimate P bound to Fe as not all compounds were identified and as the Fe_2O_3 can bind P.

Table 4: Estimating P bound to FeP in different sewage (sludge) samples (n.d. = not determined).

<u>Leeuwarden</u>	Average Line 1 & 2		Digested Sludge			
	% of total P		% of total P			
	Vivianite/FeP	Struvite/MgP	Vivianite/FeP	Struvite/MgP		
qXRD	13	43	18	35		
Mössbauer	9	-	29	-		
Elemental composition	26	36	36	25		
Sulfide	11	-	26	-		
<u>Nieuwveer</u>	A-stage Surplus sludge		B-stage Surplus Sludge		Digested Sludge	
	% of total P		% of total P		% of total P	
	Vivianite/FeP	Struvite/MgP	Vivianite/FeP	Struvite/MgP	Vivianite/FeP	Struvite/MgP
qXRD	54	0	37	0	53	0
Mössbauer	52	-	38	-	47	-
Elemental composition	55	15	43	14	59	14
Sulfide	n.d.	-	n.d.	-	31	-

4 Discussion

Significant Fe loads entered both STPs via the influent, which could originate from the municipal sewage itself, from groundwater infiltration and from Fe dosing into the sewer system (Hvitved-

Jacobsen et al., 2013; van den Kerk, 2005). This often neglected, but nevertheless, large Fe input could assist in P removal in STPs (Gutierrez et al., 2010). Despite of its significant contribution, the speciation of the influent Fe and whether it can support CPR or not was not determined. The Fe dosing in both STPs (as for most other STPs in The Netherlands) was relatively low. The molar ratios of Fe dosed to P entering via the influent was in Leeuwarden 0.13 and in Nieuwveer 0.42 (Figure 1). External Fe sources (i.e. influent and external sludge) contributed to about 80 % of the total Fe in the STP Leeuwarden. Here, a large input of Fe via the external sludge into the digester was identified. This suggests that Fe dosing can be significantly reduced, the external Fe input is sufficient to prevent H₂S emissions during anaerobic digestion. In Nieuwveer, the dosed Fe contributed more significantly to the total Fe budget, yet still 35 % of the total Fe load originated from the inflowing sewage and from external sludge.

Dissolved Fe was measured to identify equilibrium concentrations with Fe compounds. However, it turned out that during the dynamic conditions in the treatment lines of any STP (oxidizing and reducing conditions coupled to high microbial activities) measuring of a static/equilibrium Fe concentration is arbitrary. Thus, the reported dissolved Fe levels should be seen as an order of magnitude for these zones. Except for the influent and effluent samples, by far most of the Fe is part of the solid fraction. Accordingly, it was shown that even Fe(II), as product of IRB, can remain part of the solid phase (Rasmussen and Nielsen, 1996). The high dissolved Fe concentrations in the surplus sludge of the A-stage in Nieuwveer (about 30 mg Fe L⁻¹) highlighted the possibility of a slow or insufficient Fe(II) oxidation resulting in small dispersed Fe(III) and dissolved Fe(II). Sufficient oxidation and formation of Fe(III) oxides would cause a more rapid precipitation compared to Fe(II) (Ghassemi and Recht, 1971; Oikonomidis et al., 2010).

Improving the aeration of Fe(II) or dosing of Fe(III) may help to improve the limited COD removal in the A-stage of this STP (De Graaff et al., 2015).

The methodology which we employed for ammonium oxalate extraction gave only rough estimates about the Fe(II)/Fe(III) content in the sludge. The pyrophosphate extraction did not reliably extract organic Fe, as explained earlier (Stucki, 2013). In this study, Mössbauer spectroscopy was the most reliable method for quantifying and identifying Fe and FeP compounds. In contrast to XRD, Mössbauer spectroscopy can detect also amorphous Fe and FeP phases with very small particle sizes in low abundances provided appropriate standards have been prepared. On the other hand XRD detects all crystalline P compounds, also the ones that do not contain Fe. Mössbauer spectroscopy and XRD collectively showed that the solid Fe compounds of surplus sludge and anaerobic digested sludge were dominated by the ferrous phosphate mineral vivianite. Ferric iron did not play a significant role in any of the solid samples. Besides vivianite, the other major Fe compound was pyrite (Table 3).

In a membrane bioreactor with anoxic/aerobic zones, Fe(III) dominated the solid iron pool (Wu et al., 2015) also in sludge sampled from the aeration tank of an STP using Fe(II) for CPR, ammonium oxalate extraction showed that Fe(III) dominated (Rasmussen and Nielsen, 1996). However, in our samples, regardless of aerobic zone in the STPs, Fe(II) was dominant.

How is that possible? First, despite aerated areas, the sludge itself is partly non-aerated e.g. during low loading rates on weekends or in the night, in settlers and in the anoxic zones allowing the reduction of Fe(III). In flocs, oxygen free conditions can prevail throughout the treatment process due to diffusion limitation and when relatively low dissolved oxygen set-points are used. Thus, once vivianite is formed, anoxic conditions in flocs may help to channel it, without oxidation,

through the aerated nitrification zone. Both, ours (SEM-EDX) and earlier research (Frossard et al., 1997; Zelibor et al., 1988) showed that vivianite is often part of an organic matrix.

High activity of IRB in STPs has been measured which could result in rapid Fe(III) reduction and thus vivianite production (Cheng et al., 2015; Rasmussen and Nielsen, 1996). Assuming the reduction rates from Rasmussen and Nielsen, 1996, it would take between 19 h and 4 days in Leeuwarden and between 24 h and 5 days in Nieuwveer to reduce all solid Fe in the surplus sludge. These figures also indicate that Fe(III) reduction after sampling could influence the oxidation state of the Fe in samples. Once vivianite is formed, its chemical oxidation is relatively slow, on the time scale of weeks (Miot et al., 2009; Roldan et al., 2002). The oxidation by anaerobic nitrate-reducing iron-oxidizing bacteria was faster: it took approximately 16 days for complete oxidation (Miot et al., 2009). We could not find information on how long iron-oxidizing bacteria in the presence of oxygen would need for the oxidation of Fe(II) in vivianite.

In Nieuwveer and in Line 2 in Leeuwarden, where Fe(II) is dosed for CPR, the mechanisms of vivianite formation were not obvious. Vivianite could either directly precipitate from solution or formed as a result of Fe(III) reduction. Indirect chemical Fe(III) reduction, induced by e.g. sulphide, FeS_x or via humic substances (Biber et al., 1994; Golterman, 2001; Kappler et al., 2004) or direct Fe(III) reduction by IRB (Azam and Finneran, 2014; Cheng et al., 2015; Nielsen, 1996; Zhang, 2012) may have caused the formation of Fe(II) and subsequent precipitation of vivianite. Vivianite could also be precipitated directly from solution as a result of Fe(II) dosing, possibly combined with insufficient oxidation of Fe(II) (Ghassemi and Recht, 1971). In Line 1 in Leeuwarden where Fe(III) is dosed, also most of the solid Fe was present as Fe(II), mainly as vivianite. Here, chemical or biologically Fe(III) reduction must play a role. To what extent vivianite forms already in the sewer systems cannot be determined by our measurements.

When Fe(III) is used for CPR, it was suggested that first Fe(III) oxides form which cause the P removal via co-precipitation or adsorption (Smith et al., 2008). If the Fe:P ratio of these initial ferric FeP is higher than the one of vivianite (molar Fe:P=1.5) as suggested before by Fulazzaky et al., 2014 and Luedecke et al., 1989, then Fe(III) reduction and subsequent formation of vivianite can act as a net sink for P. Hence, oxidation of Fe(II) in vivianite could result in P release due to a higher molar Fe:P ratio in the formed products (Miot et al., 2009; Roldan et al., 2002). In case of FeP with a molar Fe:P of 1 (e.g. strengite), Fe(III) reduction would cause a slight net P release. However, more significant P release could only be expected when vivianite formation would be prevented as documented in the presence of sulphide when FeS_x are formed (Roden and Edmonds, 1997). Accordingly, in our experiments, addition of sulphide to the vivianite containing sludge caused a relatively quick (4 h) and significant P release.

Vivianite is very efficient in removing P from solution due to a very low solubility ($\text{p}K_{\text{sp}} \approx 36$, Al-Borno and Tomson, 1994). Fe(II) dosing for o-P removal in oxygen free conditions resulted in vivianite formation (Ghassemi, Recht 1971). The same researchers demonstrated that, in pure water, stoichiometry of o-P removal was more efficient with Fe(II) compared to Fe(III), resulting in lower residual o-P concentrations at optimum pH, and Fe(II) showed an optimum pH for o-P removal (pH=8) closer to common sewage. On the other hand, faster kinetics of Fe(III)P formation, faster settling of the formed Fe(III)P, a broader pH range for o-P removal and better COD flocculation properties were found for Fe(III) (Ghassemi and Recht, 1971; Gregory and O'Melia, 1989). In oxygen free freshwater (O'Connell et al., 2015; Rothe et al., 2014) and even in marine sediments (Jilbert and Slomp, 2013), in anoxic soils (Nanzoyo et al., 2013; Peretyazhko and Sposito, 2005) and in septic tanks (Azam and Finneran, 2014) vivianite received attention as it plays an important role in P retention (see recent review by Rothe et al., 2016). For the formation

of spherical vivianite in sediments a model has been suggested based on the presence of polymeric gel structures (Zelibor et al., 1988). At least one of the crystals we found in Nieuwveer (Figure 2B) resembles the crystals produced by Zelibor et al., 1988, indicating that the mechanism of vivianite formation could be similar in sediments and in biological STPs.

Similar to Frossard et al., 1997, with SEM-EDX we found larger crystals (up to 150 μm in diameter) with a Fe:P ratio close to the one of vivianite in digested sludge. Such large crystals were not found before digestion. The growth of the vivianite particles during digestion may be the result of the additional SRT of several weeks under constantly anaerobic conditions. Ostwaldt ripening, particle aggregation or crystal growth at elevated temperature in the digester may have caused the growth of vivianite particles/crystals. However, vivianite showed relatively slow crystal growth rates in pure solutions with higher vivianite supersaturations than observed in our samples (Madsen and Hansen, 2014) and vivianite is not stable in the presence of sulphide (Nriagu, 1972). Moreover, various inhibitors of Ostwald ripening, like DOC, are present during the digestion process. The apparent growth of vivianite particles during the digestion process is not yet fully understood.

XRD could not detect crystalline FeS_x in any of the samples analysed. Whereas Mössbauer spectroscopy revealed that pyrite contributed significantly to the solid Fe pool and even was present in the surplus sludge (9–33 % of the total Fe). The pyrite in these solids could originate from the sewer system or they were formed during the treatment process (Ingvorsen et al., 2003; Nielsen et al., 2005; van den Brand et al., 2015). Oxidation of FeS_x in STPs is on a time scale of hours (Gutierrez et al., 2010; Ingvorsen et al., 2003; Nielsen et al., 2005), it could occur in aerated zones of the STPs. However, if located in the core of the sludge flocs, FeS_x might, similar to vivianite, pass aerated zone without being oxidized.

Quantification of P bound in FeP was performed by various approaches (Table 4). Vivianite bound P contributed in Leeuwarden about 10 % before digestion and around 30 % after digestion to the total solid P, according to Mössbauer spectroscopy. The quantifications using XRD suggested, P in struvite contributes before digestion around 43 % and after digestion about 35 % of the total P. This decrease can be explained by the external input of Fe in the digester. The dissolved P concentrations are usually quite high in anaerobic digesters due to organic matter degradation and, in EBPR plants, due to the release of polyphosphates from phosphate accumulating organisms. Thus, vivianite formation is not limited by the supply of P. The Fe from the external sludge will partly react with P to form vivianite, Fe dosing to anaerobic digesters is also a measure to prevent struvite scaling as vivianite is preferably formed (Mamais et al., 1994). Some of the added Fe could react with sulphide to form FeS_x . Further P could be bound in biomass (phosphate accumulating organisms, cell material and debris) or in amorphous compounds associated with metals like Al, Mg or Ca. To be able to identify and quantify these P species would require the application of techniques like ^{31}P -NMR, sequential extraction or X-ray absorption spectroscopy (e.g. Frossard et al., 1994; Wu et al., 2015). If, however, sufficient Fe(II) is available, vivianite is expected to be the dominant inorganic solid P compound in digesters. This would make a recovery technology targeting vivianite vastly more attractive. For Nieuwveer, Mössbauer spectroscopy indicates a decrease in vivianite bound P during digestion. Here the Fe:P increases only slightly due to external sludge input. Thus, the formation of FeS_x during anaerobic digestion on expenses of vivianite causes a decrease in P bound to vivianite.

XRD might not be able to detect small particles of vivianite and amorphous FeP which Mössbauer spectroscopy does detect. We consider XRD as a semi-quantitative method. In contrast to our expectations, XRD did not underestimate the vivianite bound P and results of Mössbauer

spectroscopy were very similar (Table 4). This apparent match supports the assumption that the Fe(II) fraction in Nieuwveer, that Mössbauer spectroscopy could not clearly assign to vivianite, is actually vivianite. However, also the XRD results in Nieuwveer bear some uncertainty due to the presence of a peak that could not be assigned. Maximum quantities of P bound in FeP, AlP and MgP were estimated using the elemental composition of the TS. It was assumed that all Fe, Al and Mg is bound to P and thus other fractions of these elements were neglected. However, the elemental composition was, at least for the Fe, able to give good estimates on P bound to Fe. Sulphide was added to sample to extract P bound to Fe (Kato et al., 2006). In Leeuwarden, the sulphide extractable P fractions in digested sludge and in surplus sludge from Line 1 matched very well with P in vivianite obtained from Mössbauer spectroscopy. In Nieuwveer, the release of P from digested sludge in response to sulphide addition was much lower (31 %) compared to the P bound in vivianite (about 50 %). However, also the molar Fe:P was about 20 % lower in the sludge that was used for sulphide extraction. Translating the P release efficiency of sulphide to the sludge with the 20 % higher Fe:P ratio, we would expect a P release of about 40 %. Hence, sulphide extraction and Mössbauer spectroscopy would match better. It seems likely that the gap between sulphide extraction and the other methods is due to a difference in the sludge samples. Perhaps the released P, re-precipitated with other metals. However, from potential counter ions (Mg, Ca and Al), only Ca concentrations dropped noteworthy by 2 mmol L⁻¹ (net P release was 13 mmol L⁻¹). Or else vivianite particles were present in Nieuwveer in another form (see Mössbauer results) then the ones in Leeuwarden (e.g. more crystalline, enclosed by other minerals/organic) that made vivianite less reactive/unreactive to sulphide exposure. Overall, all methods gave good estimates for P bound to Fe and for P bound in vivianite. The elemental composition is the easiest method but gives the less accurate result. Sulphide extractions is relatively simple, here P is

released from all Fe compounds without determining the type of FeP present. XRD is a popular and common method. It allows the quantification of crystalline FeP only. In our case all Fe bound P was vivianite, hence the quantification worked well. In sludge with amorphous FeP or dispersed vivianite, XRD will not be able to quantify P bound to Fe. Mössbauer spectroscopy is, however, able to detect amorphous and crystalline Fe compounds very accurately. In Nieuwveer, about 1/3 of the Fe(II) that was assigned to vivianite could also be another Fe(II) phase. Preparation of appropriate standards may help to identify this Fe(II) using Mössbauer spectroscopy in future. In general, Mössbauer gives very accurate qualitative/quantitative results but it should be used in combination with other complementary methods like XRD.

5 Conclusion

Mössbauer spectroscopy indicated that vivianite and pyrite were the dominating solid Fe compounds in the surplus and anaerobically digested sludge from two STPs applying CPR and EBPR. XRD confirmed that vivianite was the major FeP in the samples. None of the sludge samples contained a significant amount of Fe(III) although besides Fe(II) also Fe(III) was dosed. Likely, this is related to fast iron reduction processes and slow vivianite oxidation rates. Studying Fe chemistry, helped to identify measures on how sewage treatment can be improved. In Leeuwarden, Fe dosing, to prevent sulphide emissions, can be reduced. In Nieuwveer, improving the aeration to form Fe(III) would improve COD removal in the A-stage. To assess the role of vivianite and the potential of a P recovery technology targeting on FeP, further STPs with different treatment designs (higher Fe dosing and particularly higher Fe(III) dosing) should be analysed as well. If vivianite is a general iron precipitant in STPs it could offer new routes for P recovery.

Acknowledgements

This work was performed in the TTIW-cooperation framework of Wetsus, European Centre Of Excellence For Sustainable Water Technology (www.wetsus.nl). Wetsus is funded by the Dutch Ministry of Economic Affairs, the European Union Regional Development Fund, the Province of Fryslân, the City of Leeuwarden and the EZ/Kompas program of the “Samenwerkingsverband Noord-Nederland”. We thank the participants of the research theme “Phosphate Recovery” for their financial support and helpful discussions. We acknowledge the great support by employees of Waterschap Brabantse Delta, Wetterskip Fryslan and from the two STPs.

6 References

- Al-Borno, A., Tomson, M.B., 1994. The temperature dependence of the solubility product constant of vivianite. *Geochimica et Cosmochimica Acta* 58 (24), 5373–5378.
- APHA, AWWA, WEF, 1998. Standard methods for the examination of water and wastewater, 20th ed. 1998 ed. American Public Health Association, Washington, DC.
- Azam, H.M., Finneran, K.T., 2014. Fe(III) reduction-mediated phosphate removal as vivianite ($\text{Fe}_3(\text{PO}_4)_2 \cdot 8\text{H}_2\text{O}$) in septic system wastewater. *Chemosphere* 97, 1–9.
- Biber, M.V., dos Santos Afonso, M., Stumm, W., 1994. The coordination chemistry of weathering: IV. Inhibition of the dissolution of oxide minerals. *Geochimica et Cosmochimica Acta* 58 (9), 1999–2010.
- Böhnke, B., 1977. Das Adsorptions-Belebungsverfahren. *Korrespondenz Abwasser* 24.
- Böhnke, B., Diering, B., Zuckut, S.W., 1997. Cost-effective wastewater treatment process for removal of organics and nutrients. *Water Eng. Manag.* 144 (7), 18–21.

- 663 Buffle, J., 1990. Complexation reactions in aquatic systems: an analytical approach. Ellis
664 Horwood series in analytical chemistry. Ellis Horwood.
- 665 Carliell-Marquet, C., Oikonomidis, I., Wheatley, A., Smith, J., 2009. Inorganic profiles of
666 chemical phosphorus removal sludge. *Proceedings of the ICE - Water Management* 163 (2),
667 65–77.
- 668 Carpenter, S.R., 2008. Phosphorus control is critical to mitigating eutrophication. *Pro. Natl.*
669 *Acad.Sci. USA* 105, 11039–11040.
- 670 Carpenter, S.R., Bennett, E.M., 2011. Reconsideration of the planetary boundary for phosphorus.
671 *Environ. Res. Lett.* 6 (1), 14009.
- 672 Čermáková, Z., Švarcová, S., Hradilová, J., Bezdička, P., Lančok, A., Vašutová, V., Blažek, J.,
673 Hradil, D., 2015. Temperature-related degradation and colour changes of historic paintings
674 containing vivianite. *Spectrochimica Acta Part A: Molecular and Biomolecular Spectroscopy*
675 140, 101–110.
- 676 Cheng, X., Chen, B., Cui, Y., Sun, D., Wang, X., 2015. Iron(III) reduction-induced phosphate
677 precipitation during anaerobic digestion of waste activated sludge. *Separation and Purification*
678 *Technology* 143, 6–11.
- 679 Childers, D.L., Corman, J., Edwards, M., Else, J.J., 2011. Sustainability challenges of phosphorus
680 and food: solutions from closing the human phosphorus cycle. *Bioscience* 61 (117-124).
- 681 Cline, J.D., 1969. Spectrophotometric determination of hydrosulfide in natural waters. *Limnol.*
682 *Oceogr.* 14, 454–458.
- 683 Davison, W., 1991. The solubility of iron sulphides in synthetic and natural waters at ambient
684 temperature. *Aquatic Science* 53 (4), 309–329.

- De Graaff, M., Roest, D., Brand Van Den, T., Zandvoort, M., Duin, O., van Loosdrecht, M., 2015. Characterisation of high loaded wastewater treatment processes (A-stage) to increase energy production from wastewater: performance and design guidelines. *Water research* (accepted).
- De Ridder, M., De Jong, S., Polchar, J., Lingemann, S., 2012. Risks and opportunities in the global phosphate rock market: Robust strategies in times of uncertainty. Rapport / Centre for Strategic Studies no. 17 | 12 | 12. The Hague Centre for Strategic Studies, Den Haag.
- Dyar, M.D., Jawin, E.R., Breves, E., Marchand, G., Nelms, M., Lane, M.D., Mertzman, S.A., Bish, D.L., Bishop, J.L., 2014. Mossbauer parameters of iron in phosphate minerals: Implications for interpretation of martian data. *American Mineralogist* 99 (5-6), 914–942.
- Eeckhout, S.G., Grave, E. de, Vochten, R., Blaton, N.M., 1999. Mössbauer effect study of anapaite, $\text{Ca}_2\text{Fe}^{2+}(\text{PO}_4)_2 \cdot 4\text{H}_2\text{O}$, and of its oxidation products. *Physics and Chemistry of Minerals* 26 (6), 506–512.
- El Samrani, A.G., Lartiges, B.S., Montarges-Pelletier, E., Kazpard, V., Barres, O., Ghanbaja, J., 2004. Clarification of municipal sewage with ferric chloride: The nature of coagulant species. *Water research* 38, 756–768.
- Frossard, E., Bauer, J.P., Lothe, F., 1997. Evidence of vivianite in FeSO_4 -flocculated sludges. *Water research* 31 (10), 2449–2454.
- Frossard, E., Tekely, P., Grimal, J.Y., 1994. Characterization of phosphate species in urban sewage sludges by high-resolution solid-state ^{31}P NMR. *Eur J Soil Science* 45, 403–408.
- Fulazzaky, M.A., Salim, N., Abdullah, N.H., Yusoff, A., Paul, E., 2014. Precipitation of iron-hydroxy-phosphate of added ferric iron from domestic wastewater by an alternating aerobic–anoxic process. *Chemical Engineering Journal* 253, 291–297.

- Gaffney, J.W., White, K.N., Boulton, S., 2008. Oxidation State and Size of Fe Controlled by Organic Matter in Natural Waters. *Environ. Sci. Technol.* 42 (10), 3575–3581.
- Geraarts, B., Koetse, E., Loeffen, P., Reijnders, B., Gaillard, A., 2007. Fosfaatruiming uit ijzerarm slib van rioolwaterzuiveringsinrichtingen. STOWA, 83 pp.
http://www.stowa.nl/Upload/publicaties2/mID\4924_cID\3914_74684671_STOWA 2007 31.pdf.
- Ghassemi, M., Reijnders, H.L., 1971. Phosphate Precipitation with Ferrous Iron. *Water Pollution Control Research Series*, 64 pp.
- Golterman, H.L., 2001. Phosphate release from anoxic sediments or ‘What did Mortimer really write?’. *Hydrobiologia* 450 (1/3), 99–106.
- Gonser, U., Grant, R.W., 1976. Determination of spin directions and electric fields gradient axes in vivianite by polarized recoil free γ -Rays. *Phys. Stat. Sol.* 21 (331).
- Gregory, J., O’Melia, C.R., 1989. Fundamentals of flocculation. *Critical Reviews in Environmental Control* 19 (3), 185–230.
- Gutierrez, O., Park, D., Sharma, K.R., Yuan, Z., 2010. Iron salts dosage for sulfide control in sewers induces chemical phosphorus removal during wastewater treatment. *Water research* 44 (11), 3467–3475.
- Harker, S.J., Pollard, R.J., 1993. A study of magnetite at 4.2 K and subject to strong applied magnetic fields. *Nuclear Instruments and Methods in Physics Research Section B: Beam Interactions with Materials and Atoms* 76 (1-4), 61–63.
- Higgins, M., Murthy, S., 2006. Understanding factors affecting polymer demand for thickening and dewatering. Water Environment Research Foundation; IWA Publishing, Alexandria, Va, London.

- Hsu, P.H., 1976. Comparison of iron(III) and aluminum in precipitation of phosphate from solution. *Water research* 10 (10), 903–907.
- Hvitved-Jacobsen, T., Vollertsen, J., Nielsen, A.H., 2013. *Sewer processes: Microbial and chemical process engineering of sewer networks*, 2nd ed. ed. CRC Press, Boca Raton.
- Ingvorsen, K., Nielsen, M.Y., Joulain, C., 2003. Kinetics of bacterial sulfate reduction in an activated sludge plant. *Microb Ecol* 46, 129–137.
- Jackson, A., Gaffney, J.W., Boulton, S., 2012. Subsurface interactions of Fe(II) with humic acid or landfill leachate do not control subsequent iron(III) (hydr)oxide production at the surface. *Environ. Sci. Technol.* 46 (14), 7543–7550.
- Jetten, M., Horn, S., van Loosdrecht, M.C.M., 1997. Towards a more sustainable municipal wastewater treatment system. *Water Science & Technology* 35 (9), 171–180.
- Jilbert, T., Slomp, C.P., 2013. Iron and manganese shuttles control the formation of authigenic phosphorus minerals in the euxinic basins of the Baltic Sea. *Geochimica et Cosmochimica Acta* 107, 155–169.
- Kappler, A., Benz, M., Schink, B., Brune, A., 2004. Electron shuttling via humic acids in microbial iron(III) reduction in a freshwater sediment. *FEMS Microbiology Ecology* 47 (1), 85–92.
- Kato, F., Kitakoji, H., Oshita, K., Takaoka, M., Takeda, N., Matsumoto, T., 2006. Extraction efficiency of phosphate from pre-coagulated sludge with NaHS. *Water Science & Technology* 54 (5), 119.
- Klencsár, Z., 1997. Mössbauer spectrum analysis by Evolution Algorithm. *Nuclear Instruments and Methods in Physics Research Section B: Beam Interactions with Materials and Atoms* 129 (4), 527–533.

- Kraal, P., Slomp, C.P., Forster, A., Kuypers, M., Sluijs, A., 2009. Pyrite oxidation during sample storage determines phosphorus fractionation in carbonate-poor anoxic sediments. *Geochimica et Cosmochimica Acta* 73, 3277–3290.
- Kracht, O., Gresch, M., Gujer, W., 2007. A Stable Isotope Approach for the Quantification of Sewer Infiltration. *Environ. Sci. Technol.* 41 (16), 5839–5845.
- Leavens, P.B. (Ed.), 1972. Oxidation of vivianite in New Jersey Cretaceous greensands.
- Li, J., 2005. Effects of Fe(III) on floc characteristics of activated sludge. *J. Chem. Technol. Biotechnol.* 80 (3), 313–319.
- Luedecke, C., Hermanowicz, S.W., Jenkins, D., 1989. Precipitation of ferric phosphate in activated-sludge - A chemical model and its verification. *Water Science & Technology* 21 (4-5), 325–337.
- Macdonald, G.K., Bennett, E.M., Potter, P.A., Ramankutty, N., 2011. Agronomic phosphorus imbalances across the world's croplands 108 (7), 3086–3091.
- Madsen, H., Hansen, H., 2014. Kinetics of crystal growth of vivianite, $\text{Fe}_3(\text{PO}_4)_2 \times 8\text{H}_2\text{O}$, from solution at 25, 35 and 45 °C. *Journal of Crystal Growth* (401), 82–86.
- Mamais, D., Pitt, P.A., Cheng, Y.W., Loiacono, J., Jenkins, D., 1994. Determination of ferric chloride dose to control struvite precipitation in anaerobic sludge digesters. *Water Environ Res* 66 (7), 912–918.
- McKeague, J.A., 1967. An evaluation of 0.1 M pyrophosphate and pyrophosphate-dithionite in comparison with oxalate as extractants of accumulation products in podzols and some other soils. *Can. J. Soil. Sci.* 47 (2), 95-&.

- 774 Miot, J., Benzerara, K., Morin, G., Bernard, S., Beyssac, O., Larquet, E., Kappler, A., Guyot, F.,
 775 2009. Transformation of vivianite by anaerobic nitrate-reducing iron-oxidizing bacteria.
 776 *Geobiology* 7 (3), 373–384.
- 777 Mullet, M., Boursiquot, S., Abdelmoula, M., Génin, J.M., Ehrhardt, J.J., 2002. Surface chemistry
 778 and structural properties of mackinawite prepared by reaction of sulfide ions with metallic
 779 iron. *Geochimica et Cosmochimica Acta* 66 (5), 829–836.
- 780 Murad, E., Cashion, J., 2004. Mössbauer Spectroscopy of Environmental Materials and Their
 781 Industrial Utilization. Springer US, Boston, MA.
- 782 Nanzyo, M., Onodera, H., Hasegawa, E., Ito, K., Kanno, H., 2013. Formation and Dissolution of
 783 Vivianite in Paddy Field Soil. *Soil Science Society of America Journal* 77 (4), 1452.
- 784 Nielsen, A.H., Lens, P., Vollertsen, J., Hvitved-Jacobsen, T., 2005. Sulfide–iron interactions in
 785 domestic wastewater from a gravity sewer. *Water research* 39 (12), 2747–2755.
- 786 Nielsen, J.L., Nielsen, P.H., 1998. Microbial Nitrate-Dependent Oxidation of Ferrous Iron in
 787 Activated Sludge. *Environ. Sci. Technol.* 32, 3556–3561.
- 788 Nielsen, P., 1996. The significance of microbial Fe(III) reduction in the activated sludge process.
 789 *Water Science & Technology* 34 (5-6), 129–136.
- 790 Nriagu, J.O., 1972. Stability of vivianite and ion-pair formation in the system $\text{Fe}_3(\text{PO}_4)_2$ -
 791 H_3PO_4 - H_2O . *Geochimica et Cosmochimica Acta* 36 (4), 459–470.
- 792 O'Connell, D.W., Jensen, M.M., Jakobsen, R., Thamdrup, B., Andersen, T.J., Kovacs, A., Hansen,
 793 H., 2015. Vivianite formation and its role in phosphorus retention in Lake Ørn, Denmark.
 794 *Chemical Geology* 409, 42–53.
- 795 Oikonomidis, I., Burrows, L.J., Carliell-Marquet, C., 2010. Mode of action of ferric and ferrous
 796 iron salts in activated sludge. *J. Chem. Technol. Biotechnol.* 85 (8), 1067–1076.

- Paul, E., Laval, M.L., Sperandio, M., 2001. Excess sludge production and costs due to phosphorus removal. *Environmental technology* 22, 1363–1371.
- Peretyazhko, T., Sposito, G., 2005. Iron(III) reduction and phosphorous solubilization in humid tropical forest soils. *Geochimica et Cosmochimica Acta* 69 (14), 3643–3652.
- Poffet, M.S., 2007. Thermal runaway of the dried sewage sludge in the storage tanks: from molecular origins to technical measures of smouldering fire prevention. Dissertation thesis.
- Rasmussen, H., Nielsen, P., 1996. Iron reduction in activated sludge measured with different extraction techniques. *Water research* 30 (3), 551–558.
- Recht, H.L., Ghassemi, M., 1970. Kinetics and mechanism of precipitation and nature of the precipitate obtained in phosphate removal from wastewater using aluminum(III) and iron(III) salts. *Water Pollution Control Research Series*. U.S. Dept. of the Interior, FWQA.
- Roden, E.E., Edmonds, J.W., 1997. Phosphate mobilization in iron-rich anaerobic sediments: Microbial Fe(III) oxide reduction versus iron-sulfide formation. *Archiv für Hydrobiologie* 139 (3), 347–378.
- Roldan, R., Barron, V., Torrent, J., 2002. Experimental alteration of vivianite to lepidocrocite in a calcareous medium. *clay miner* 37 (4), 709–718.
- Rothe, M., Frederichs, T., Eder, M., Kleeberg, A., Hupfer, M., 2014. Evidence for vivianite formation and its contribution to long-term phosphorus retention in a recent lake sediment: A novel analytical approach. *Biogeosciences* 11 (18), 5169–5180.
- Rothe, M., Kleeberg, A., Hupfer, M., 2016. The occurrence, identification and environmental relevance of vivianite in waterlogged soils and aquatic sediments. *Earth-Science Reviews* 158, 51–64.

- Scholz, R.W., Wellmer, F.W., 2016. Comment on: "Recent revisions of phosphate rock reserves and resources: a critique" by Edixhoven et al. (2014) – clarifying comments and thoughts on key conceptions, conclusions and interpretation to allow for sustainable action. *Earth Syst. Dynam.* 7 (1), 103–117.
- Seitz, M.A., Riedner, R.J., Malhotra, S.K., Kipp, R.J., 1973. Iron-phosphate compound identification in sewage sludge residue. *Environ. Sci. Technol.* 7 (4), 354–357.
- Siegrist, H., Salzgeber, D., Eugster, J., Joss, A., 2008. Anammox brings WWTP closer to energy autarky due to increased biogas production and reduced aeration energy for N-removal. *Water Science & Technology* 57 (3), 383–388.
- Singer, P.C., 1972. Anaerobic control of phosphate by ferrous iron: Anaerobic control of phosphate by ferrous iron. *Journal Water Pollution Control Federation* 44 (4), 663-&.
- Sklute, E.C., Jensen, H.B., Rogers, A.D., Reeder, R.J., 2015. Morphological, structural, and spectral characteristics of amorphous iron sulfates. *J. Geophys. Res. Planets* 120 (4), 809–830.
- Smith, S., Takacs, I., Murthy, S., Daigger, G.T., Szabo, A., 2008. Phosphate complexation model and its implications for chemical phosphorus removal. *Water Environ Res* 80 (5), 428–438.
- Stucki, J.W., 2013. *Iron in soils and clay minerals*. Springer, [Place of publication not identified].
- Szabó, A., Takács, I., Murthy, S., Daigger, G.T., Licskó, I., Smith, S., 2008. Significance of Design and Operational Variables in Chemical Phosphorus Removal. *Water Environ Res* 80 (5), 407–416.
- Takács, I., Murthy, S., Smith, S., McGrath, M., 2006. Chemical phosphorus removal to extremely low levels: experience of two plants in the Washington, DC area. *Water Science & Technology* 53 (12), 21.

- Tchobanoglous, G., Burton, F.L., Stensel, H.D., 2013. Wastewater engineering: Treatment and reuse, 5th ed. ed. McGraw-Hill Higher Education; McGraw-Hill [distributor], New York, London.
- Thomas, A.E., 1965. Phosphat-Elimination in der Belebtschlammanlage von Männedorf und Phosphat-Fixation in See- und Klärschlamm. Vierteljahrschr. Naturforsch. Ges. Zürich 110, 419–434.
- van den Brand, T. P. H., Roest, K., Chen, G. H., Brdjanovic, D., van Loosdrecht, M. C. M., 2015. Occurrence and activity of sulphate reducing bacteria in aerobic activated sludge systems. World J Microbiol Biotechnol 31 (3), 507–516.
- van den Kerk, A.J., 2005. Vervolgonderzoek rioolvreemd water. STOWA, Utrecht.
- van Dijk, K.C., Lesschen, J.P., Oenema, O., 2016. Phosphorus flows and balances of the European Union Member States. Science of The Total Environment 542, 1078–1093.
- van Hullebusch, E.D., Utomo, S., Zandvoort, M., Lens, P., 2005. Comparison of three sequential extraction procedures to describe. Talanta 65, 549–558.
- Verschoor, M.J., Molot, A.M., 2013. A comparison of three colorimetric methods of ferrous and total reactive iron measurement in freshwaters (11), 113–125.
- Viollier, E., Inglett, P.W., Hunter, K., Roychoudhury, A.N., van Cappellen, P., 2000. The ferrozine method revisited: Fe(II)/Fe(III) determination in natural waters. Applied Geochemistry 15 (6), 785–790.
- Walan, P., Davidsson, S., Johansson, S., Höök, M., 2014. Phosphate rock production and depletion: Regional disaggregated modeling and global implications. Resources, Conservation and Recycling 93, 178–187.

- 863 WEF, 2011. Nutrient removal. WEF manual of practice no. 34. McGraw-Hill; WEF Press, New
864 York, Alexandria, Va.
- 865 Wilfert, P., Suresh Kumar, P., Korving, L., Witkamp, G.J., van Loosdrecht, M.C.M., 2015. The
866 relevance of phosphorus and iron chemistry to the recovery of phosphorus from wastewater: a
867 review. *Environ. Sci. Technol.*
- 868 Wolf, A.M., Moore, P.A., Kleinman, P., Sullivan, D.M., 2009. Water-Extractable Phosphorus in
869 Animal Manure and Biosolids, in: , *Methods for Phosphorus Analysis for Soils, Sediments,*
870 *Residuals, and Waters*, pp. 76–80.
- 871 Wu, H., Ikeda-Ohno, A., Wang, Y., Waite, T.D., 2015. Iron and phosphorus speciation in Fe-
872 conditioned membrane bioreactor activated sludge. *Water research* 76, 213–226.
- 873 Yoshida, Y., Langouche, G. (Eds.), 2013. *Mossbauer spectroscopy: Tutorial book*. Springer,
874 Berlin, New York.
- 875 Zelibor, J.L., Senftle, F.E., Reinhardt, J.L., 1988. A proposed mechanism for the formation of
876 spherical vivianite crystal aggregates in sediments. *Sedimentary Geology* 59 (1-2), 125–142.
- 877 Zhang, X., 2012. Factors Influencing Iron Reduction–Induced Phosphorus Precipitation.
878 *Environmental Engineering Science* 29 (6), 511–519.

879 7 Supporting information

ACCEPTED MANUSCRIPT

880 Table A. 1: Measured parameters in the STP Leeuwarden. The reported values are the mean and the standard deviation of the three measurement
 881 campaigns between December 2013 and February 2014. In each campaign all measurements were made in triplicates. The Effluent from line 2
 882 was only measured once.

LWD	T (°C)	pH	ORP (mV)	TS (g/kg)	VS (g/kg)	TA (mEq/L)	Fe(II) (mg/L)	Fe(III) (mg/L)	Total Dissolved Fe-Ferrozine (mg/L)	Total Dissolved Fe-ICP (mg/L)	Total Fe (mg/kg)	Total Solid Fe (mg/g TS)	o-P (mg P/L)	Total Dissolved P (mg/L)	Total P (mg/kg)	Total Solid P (mg/g TS)	S-SO4 (mg S/L)	Total Dissolved S (mg/L)	Total S (mg/kg)	Total Solid S (mg/g TS)
Influent	11.6 (4.6)	7.9 (0.1)	-195 (61)	1.2 (0.2)	0.4 (0.1)	10.4 (4.4)	0	0.3	0.3 (0)	0.2 (0.1)	1.7 (0.4)	1.2 (0.2)	4.5 (2.8)	5.3 (3.1)	7.5 (3.8)	2.1 (1)	9.6 (1.9)	9.4 (3.1)	18.2 (8.3)	7.5 (7.6)
Effluent line 1	11.2 (1.6)	7.6 (0.2)	62 (63)	0.7 (0.2)	0.1 (0.0)	6.9 (0.5)	0	0.1	0.1 (0.1)	0.1 (0.0)	0.3 (0.1)	0.1 (0.1)	0.4 (0.3)	0.5 (0.4)	0.9 (0.4)	0.5 (0.4)	11 (1.2)	10.5 (1.2)	15.7 (5.5)	8.4 (10.2)
Effluent line 2	12.2	7.8	45	0.9	0.1 (n.d.)	5.6 (n.d.)	0	0.1	0.1	0.1	0.5	0.4	0.2	0.3	0.4	0.2	12.4	13	13.6	0.7
Before Fe dosing line 2	11.4 (4.6)	7.4 (0.1)	-156 (35)	4.2 (0.1)	3 (0.2)	9.1 (1.5)	0.1	0.6	0.7 (0.3)	0.7 (0.3)	52.5 (9.5)	12.2 (2.0)	10.1 (9.9)	11.2 (10.4)	109.8 (16.9)	23.4 (1.4)	11 (1.8)	10.1 (2.6)	38 (1.8)	6.6 (0.6)
After Fe dosing line 2	11.7 (4.5)	7.3 (0.0)	-18 (40)	4.7 (0.4)	3.2 (0.3)	7.6 (0.9)	0.1	0.5	0.6 (0.3)	0.5 (0.3)	59.1 (16.3)	12.7 (3.7)	1.6 (0.6)	2 (0.8)	119.8 (19.9)	25.2 (2.2)	11.3 (1)	10.4 (2.5)	41.8 (10.1)	6.7 (1.8)
Surplus sludge line 1	12.3 (2.7)	7.4 (0.1)	-42 (75)	69 (0.7)	4.9 (0.7)	8.9 (0.7)	0.1	0.5	0.6 (0.1)	0.5 (0.1)	106.4 (25.2)	15.3 (2.7)	2.7 (1.2)	3.4 (1.4)	188.9 (9.1)	27.1 (2.2)	11.4 (1.2)	10.5 (2.1)	53.9 (5.1)	6.4 (0.4)
Surplus sludge line 2	12.4 (3.7)	7.3 (0.0)	-90 (8)	69 (0.3)	4.9 (0.1)	9.5 (0.7)	0.6	0.6	1.1 (0.3)	1.2 (0.4)	96.8 (37.8)	13.8 (4.9)	4.3 (0.4)	5.6 (0.0)	192 (5.7)	26.9 (0.6)	11.2 (1.6)	11 (3.5)	58.3 (8.3)	6.9 (0.4)
Digested sludge	29.3 (0.2)	7.4 (0.1)	-380 (27)	45.6 (0.7)	28.4 (0.8)	157.8*/211.7** (11.9/30.8)	0.6	1.6	2.1 (0.2)	1.7 (0.4)	1849.7 (92.3)	40.5 (1.9)	169.6 (22.4)	179.3 (33.6)	1970.6 (149.1)	39.4 (3.3)	5.1 (2.4)	7.1 (1.8)	418.5 (21.6)	9 (0.4)

*Supernatant after centrifugation

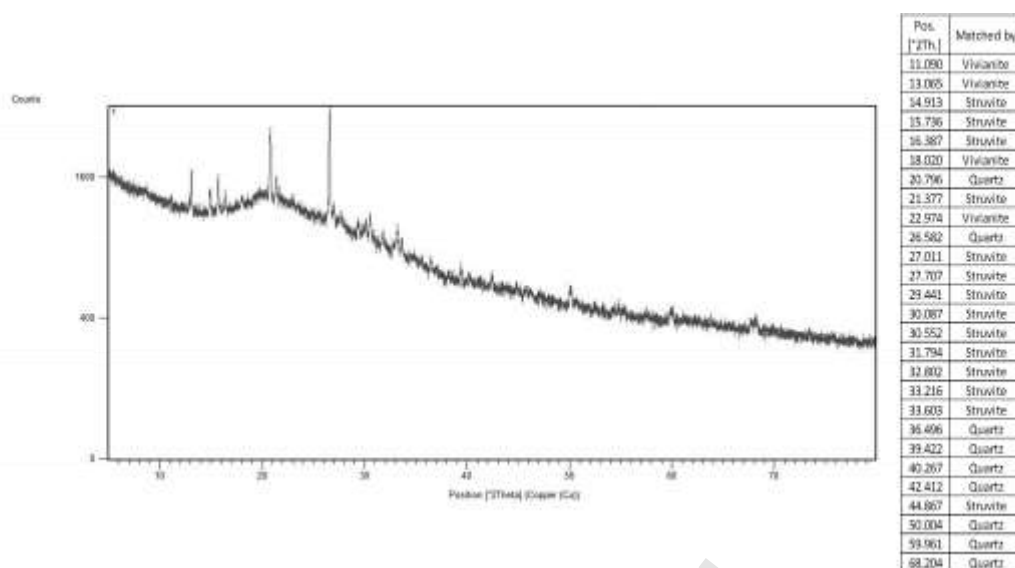
** Raw sludge

LWD	Total Dissolved Al (mg/L)	Total Al (mg/kg)	Total Solid Al (mg/g TS)	Total Dissolved Mg (mg/L)	Total Mg (mg/kg)	Total Solid Mg (mg/g TS)	Total Dissolved Ca (mg/L)	Total Ca (mg/kg)	Total Solid Ca (mg/g TS)	Total Dissolved K (mg/L)	Total K (mg/kg)	Total Solid K (mg/g TS)	Total Dissolved Na (mg/L)	Total Na (mg/kg)	Total Solid Na (mg/g TS)
Influent	<0.1	<1.25	-	12.3 (0.7)	13.9 (2.4)	1.7 (2.4)	64.1 (12.3)	75 (9.7)	10.6 (9.3)	20.6 (9.8)	25.8 (14.6)	4.5 (4.1)	178.6 (43.8)	213.6 (14.6)	34.1 (29.9)
Effluent line 1	<0.05	<1.25	-	10.3 (1.6)	11 (1.6)	1.1 (0.6)	58.4 (11.2)	64 (9)	8.8 (4.9)	13.5 (2)	15.4 (2.8)	2.2 (2.9)	164.3 (48.2)	173.5 (45.7)	14 (7.3)
Effluent line 2	<0.05	<1.25	-	12.9	13.2	0.3	72.4	75.2	3.3	13.2	17.4	4.8	194.5	201	7.7
Before Fe dosing line 2	<0.2	21.2 (1.2)	5 (0.4)	13.6 (1.5)	34.4 (1.8)	4.9 (0.1)	59.8 (15.9)	151.3 (17.6)	21.7 (7.4)	21.1 (7.4)	54.1 (2.1)	7 (1.2)	168.1 (61.7)	181.8 (61.9)	3.4 (1.1)
After Fe dosing line 2	<0.1	23 (1.5)	5 (0.6)	11.7 (1.6)	36.9 (3.7)	5.4 (0.6)	61 (12.2)	158.2 (22.2)	20.7 (3.9)	16.2 (1.9)	57.64 (2.7)	36.8 (49.1)	154.3 (43.6)	168.2 (46.6)	3.1 (0.8)
Surplus sludge line 1	<0.2	34.3 (7.9)	5 (0.7)	11.8 (1.5)	50.5 (2)	5.7 (0.7)	58.8 (10.8)	207.8 (11.3)	22 (3.8)	18.1 (0.3)	78.7 (5.4)	25 (27.2)	168.2 (50.4)	191.5 (43.4)	3.6 (1.3)
Surplus sludge line 2	< 0.2	34.7 (7.6)	5 (0.9)	13 (2.9)	51 (3)	5.5 (0.2)	59.8 (15.6)	205.8 (0.4)	21.3 (3.1)	19.8 (1)	76.7 (10.0)	8.3 (1.0)	163.7 (47.1)	171.8 (45.0)	1.3 (0.3)
Digested sludge	<0.5	239.8 (17.4)	5.3 (0.4)	5.4 (4.5)	370.8 (37.5)	8 (0.8)	49.9 (5.2)	1901 (183.7)	40.6 (3.5)	500.4 (29.2)	551.4 (29.0)	1.6 (0.6)	263.2 (12.2)	289.8 (49.5)	0.8 (0.8)

Table A. 2: Measured parameters in the STP Nieuwveer. Nieuwveer was only sampled once in March 2014. The reported values are the mean and standard deviation of triplicate measurements.

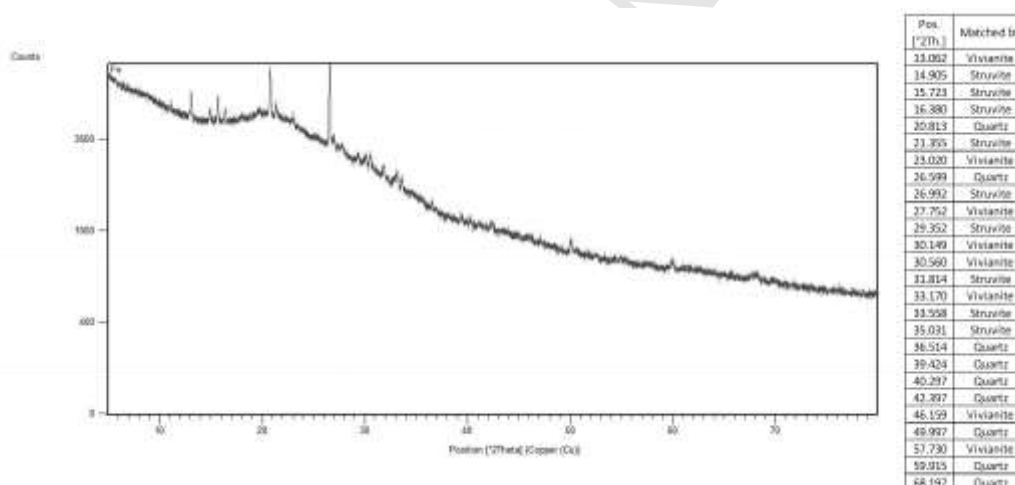
Nieuwveer	T (°C)	pH	ORP (mV)	TS (g/kg)	VS (g/kg)	TA (mEq/L)	Fe(II) (mg/L)	Fe(III) (mg/L)	Total Dissolved Fe-Ferrozine (mg/L)	Total Dissolved Fe-ICP (mg/L)	Total Fe (mg/kg)	Total Solid Fe (mg/g TS)	o-P (mg P L ⁻¹)	Total Dissolved P (mg/L)	Total P (mg/kg)	Total Solid P (mg/g TS)	SO ₄ (mg S L ⁻¹)	Total Dissolved S (mg/L)	Total S (mg/kg)	Total Solid S (mg/g TS)
Influent	9.8	7.3	10	0.4 (0.01)	0.1 (0.01)	4.6	0	0.3 (0.0)	0.3 (0.0)	0.2	0.86 (0.0)	1.4	1.6	2.0	2.9 (0.0)	2.3	10.8	10.8	11.3 (0.2)	1.4
Effluent	9.7	7	117	0.3 (0.02)	0.08 (0.0)	2.1	0.0	0.1 (0.0)	0.09 (0.0)	0.1	0.23 (0.0)	0.5	0.8	1.1	1.3 (0.0)	0.7	10.8	9.9	10.4 (0.1)	1.6
A-stage	9.4	7.1	-90	3.6 (0.1)	2.8 (0.1)	11.8	0.0	0.8 (0.1)	0.8 (0.1)	0.8	82.5 (2.1)	22.4	1.0	1.5	57.7 (0.5)	15.4	12.0	11.2	20.9 (2.1)	2.7
A-stage: Surplus sludge	10	6.8	-264	18.6 (0.1)	14.8 (0.1)	13.2	18.3 (1.1)	12.7 (0.1)	31 (1.2)	32.4	436.7 (23.6)	21.8	18.9	31.2	290.2 (15.3)	13.9	10.0	16.8	89.5 (2.6)	3.9
B-stage: Surplus sludge	9.4	7	-109	14.9 (0.3)	11.6 (0.2)	9.1	0.0	1.9 (0.0)	1.9 (0.03)	1.4	426.7 (9.4)	28.6	5.5	7.2	375 (7.1)	24.8	10.9	11.4	107.8 (3.5)	6.5
External sludge before digestion	17	6	-294	75.9 (8.1)	58.3 (5.9)	30.2	70.7 (1.2)	26.8 (26.9)	97.6 (7.8)	90.0	1747 (139)	21.8	12.9	54.8	1121.8 (82.9)	14.1	18.6	15.3	347 (21.6)	4.4
Digested sludge	27	7.7	-322	41.6 (0.1)	24.8 (0.7)	140.7	0.1 (0.0)	3.0 (0.1)	3.1 (0.1)	3.0	2389 (78.7)	57.4	70.2	73.8	1558.2 (29.2)	35.8	7.1	14.5	442.2 (8.4)	10.3

Nieuwveer	Total Dissolved Al (mg/L)	Total Al (mg/kg)	Total Solid Al (mg/g TS)	Total Dissolved Mg (mg/L)	Total Mg (mg/kg)	Total Solid Mg (mg/g TS)	Total Dissolved Ca (mg/L)	Total Ca (mg/kg)	Total Solid Ca (mg/g TS)	Total Dissolved K (mg/L)	Total K (mg/kg)	Total Solid K (mg/g TS)	Total Dissolved Na (mg/L)	Total Na (mg/kg)	Total Solid Na (mg/g TS)
Influent	<0.1	0.3 (0.0)	0.9	5.2	5.6 (0.0)	1.2	44.0	45.7 (0.1)	4.7	14.0	14.6 (0.2)	1.5	48.8	47.1 (0.2)	-
Effluent	<0.05	<0.2	-	4.5	4.7 (0.1)	0.7	37.3	37.9 (0.5)	2.2	11.2	12.9 (0.2)	5.5	43.6	42.7 (0.7)	-
A-stage	<0.5	19.4 (1.6)	5.3	4.7	<17	-	40.3	143.3 (5.2)	28.3	13.1	34.8 (0.7)	6	45.4	<83	-
A-stage: Surplus sludge	<0.2	82.2 (7.3)	4.4	10.7	39.7 (2.8)	1.6	88.5	373.3 (23.6)	15.4	34.7	69.7 (4.7)	1.9	56.7	<83	-
B-stage: Surplus sludge	<0.2	77.5 (1.2)	5.2	5.6	46 (0.9)	2.7	39.8	309.5 (10.1)	18.2	20.5	100.5 (4.9)	5.4	44.4	<83	-
External sludge before digestion	<0.5	451.5 (50.4)	5.9	34.2	137.2 (4.6)	1.4	215.5	1226.4 (40.5)	13.5	107.5	252.3 (12.4)	2	62.5	<170	-
Digested sludge	<0.5	479.9 (5.2)	11.5	12.5	170.9 (4.2)	3.8	41.8	1251.2 (13.9)	29.1	196.0	267.3 (2.5)	1.9	81.1	<160	-



890

891 *Figure A. 1: XRD diffractogram including peak list and peak assignment for surplus sludge solids sampled*
 892 *in Line 1 (Fe(III) dosing) in Leeuwarden.*



893

894 *Figure A. 2: XRD diffractogram including peak list and peak assignment for activated sludge solids*
 895 *sampled in Line 2 (Fe(II) dosing) in Leeuwarden.*

896

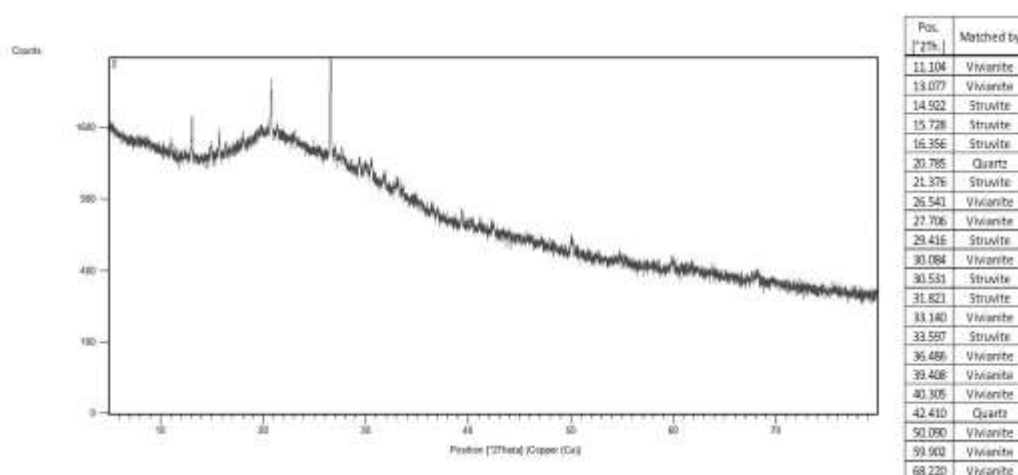


Figure A. 3: XRD diffractogram including peak list and peak assignment for surplus sludge solids sampled in Line 2 (Fe(II) dosing) in Leeuwarden.

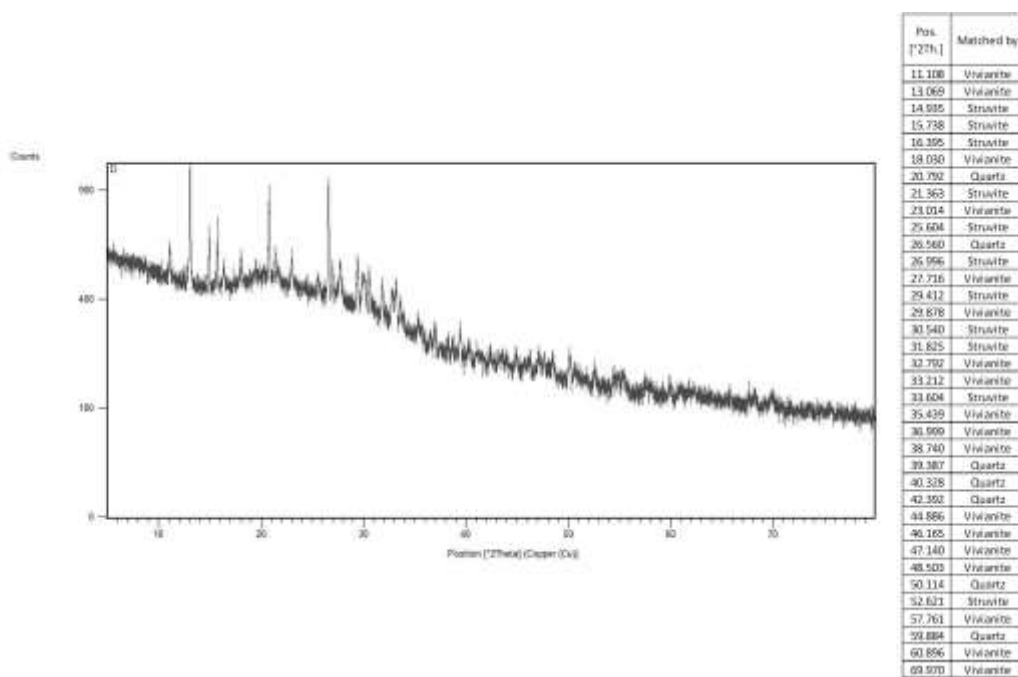


Figure A. 4: XRD diffractogram including peak list and peak assignment for digested sludge solids sampled in Leeuwarden.

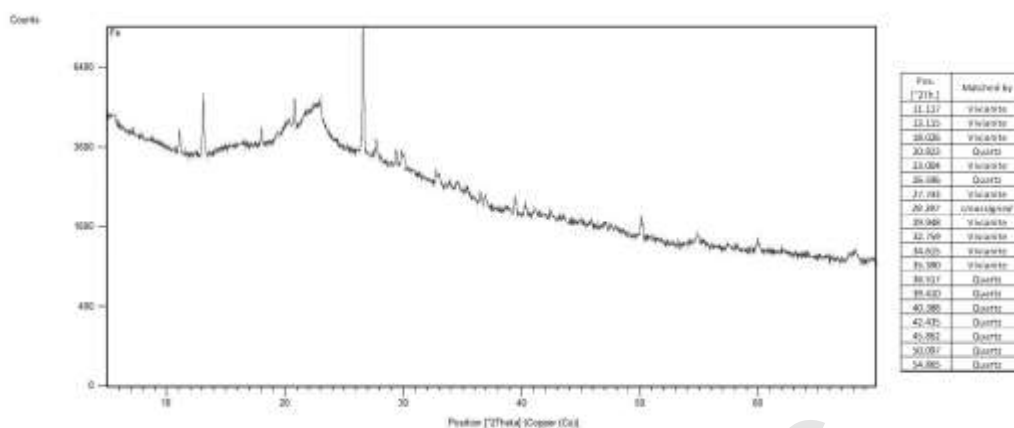


Figure A. 5: XRD diffractogram including peak list and peak assignment for A-stage sludge solids sampled directly after Fe(II) dosing in Nieuwveer.

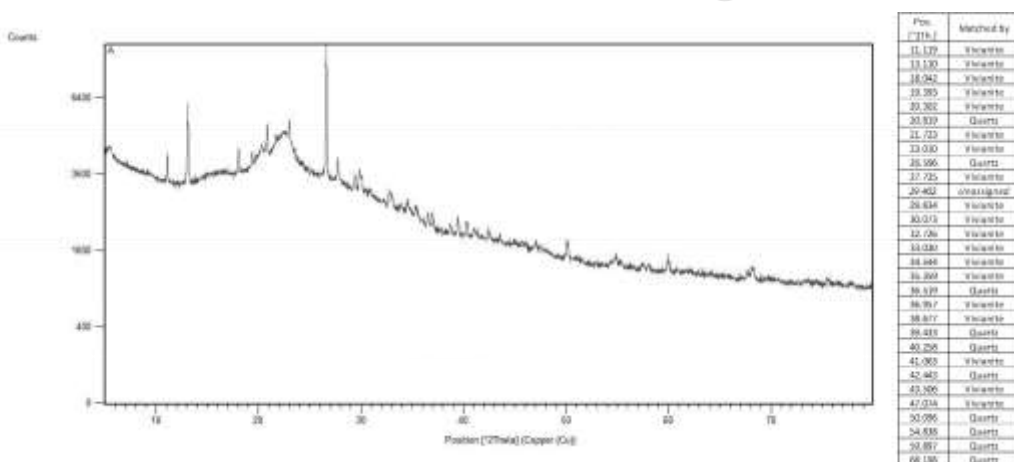


Figure A. 6: XRD diffractogram including peak list and peak assignment for surplus A-stage sludge solids sampled in Nieuwveer.

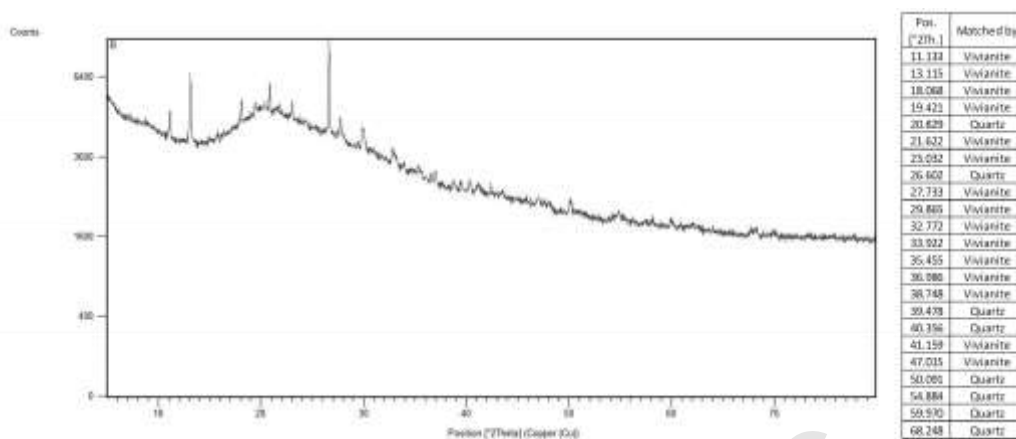


Figure A. 7: XRD diffractogram including peak list and peak assignment for surplus B-stage sludge solids sampled in Nieuwveer.

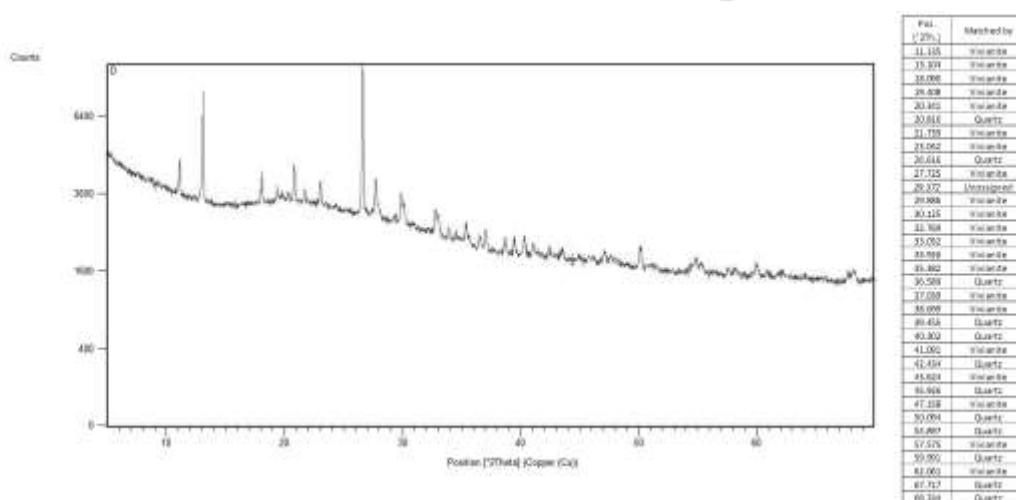


Figure A. 8: XRD diffractogram including peak list and peak assignment for digested sludge solids sampled in Nieuwveer.

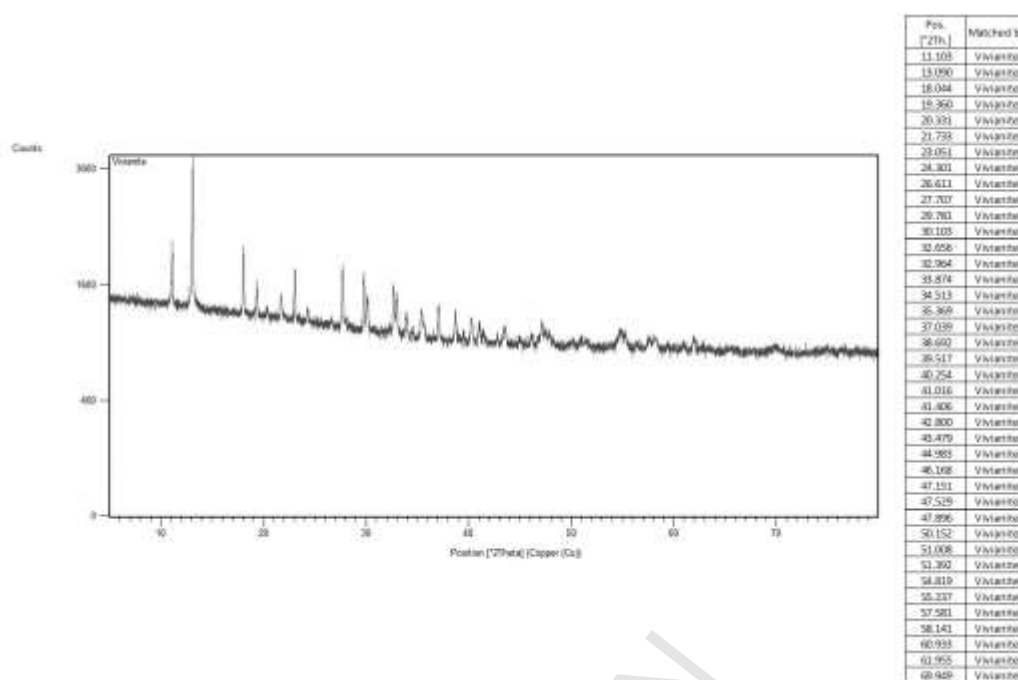


Figure A. 9: XRD diffractogram including peak list and peak assignment for the vivianite standard.

Table A. 3: Results of Mössbauer measurements at 300 K.

Sample	IS (mm·s ⁻¹)	QS (mm·s ⁻¹)	Hyperfine field (T)	Γ (mm·s ⁻¹)	Phase	Spectral contribution (%)
Leeuwarden Line 1 (Fe(III) dosing)	0.27	0.84	-	0.50	Fe ³⁺	57
	1.28	2.40	-	0.36	Fe ²⁺	20
	1.49	2.58	-	0.38	Fe ²⁺	17
	1.36	0.96	-	0.31	Fe ²⁺	6
Leeuwarden Line 2 (Fe(II) dosing)	0.28	0.87	-	0.49	Fe ³⁺	56
	1.24	2.36	-	0.30	Fe ²⁺	19
	1.47	2.53	-	0.34	Fe ²⁺	18
	1.22	1.13	-	0.28	Fe ²⁺	7
Leeuwarden digested solids	0.27	0.93	-	0.54	Fe ³⁺	62
	1.17	2.46	-	0.32	Fe ²⁺	14
	1.44	2.57	-	0.39	Fe ²⁺	24
Nieuwveer A-stage solids	0.20	0.89	-	0.31	Fe ³⁺	11
	1.08	2.67	-	0.30	Fe ²⁺	33
	1.31	2.74	-	0.34	Fe ²⁺	56
Nieuwveer B-stage solids	0.31	0.85	-	0.48	Fe ³⁺	44
	1.08	2.66	-	0.33	Fe ²⁺	21
	1.39	2.57	-	0.39	Fe ²⁺	35
Nieuwveer digested solids	0.30	0.91	-	0.51	Fe ³⁺	45
	1.07	2.66	-	0.32	Fe ²⁺	19
	1.37	2.64	-	0.39	Fe ²⁺	36
Vivianite Standard	0.23	1.09	-	0.41	Fe ³⁺	20
	1.27	2.33	-	0.42	Fe ²⁺	28
	1.27	2.87	-	0.42	Fe ²⁺	52

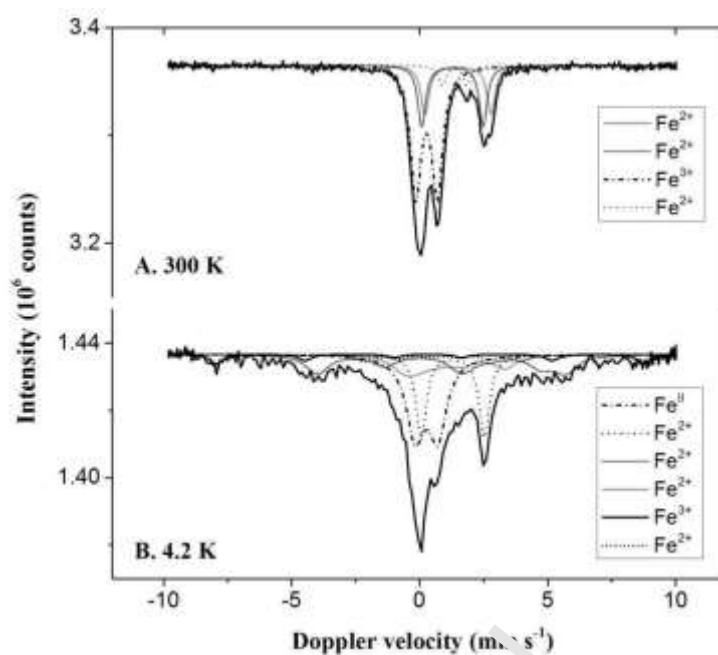


Figure A. 10: Mössbauer spectra obtained at different temperatures with the surplus sludge solids sampled in Line 1 (Fe(III) dosing) in Leeuwarden.

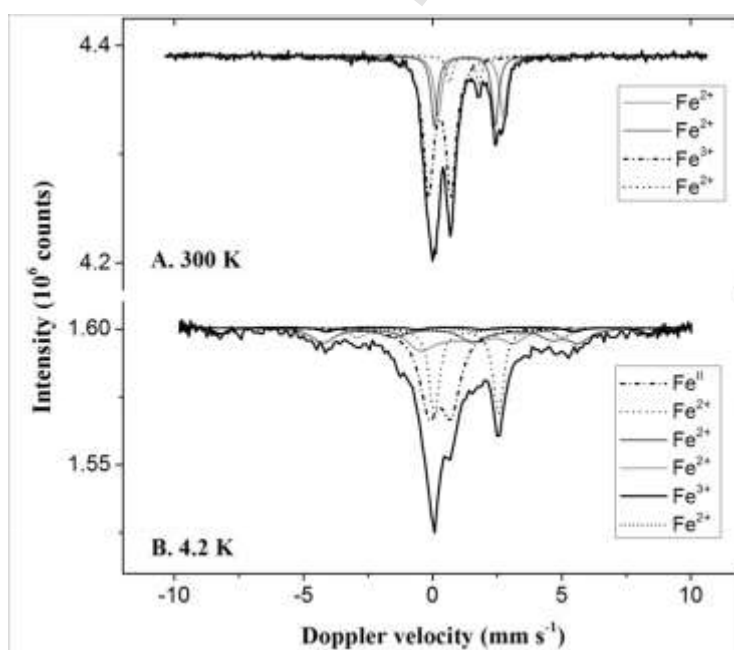
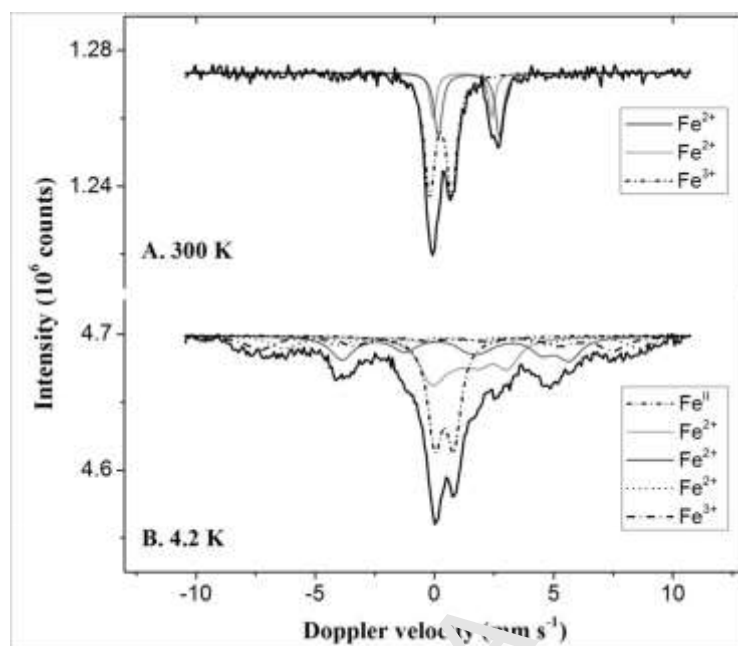


Figure A. 11: Mössbauer spectra obtained at different temperatures with the surplus sludge solids sampled in Line 2 (Fe(II) dosing) in Leeuwarden.

929



930

931 *Figure A. 12: Mössbauer spectra obtained at different temperatures with the digested sludge solids*
 932 *sampled in Leeuwarden.*

933

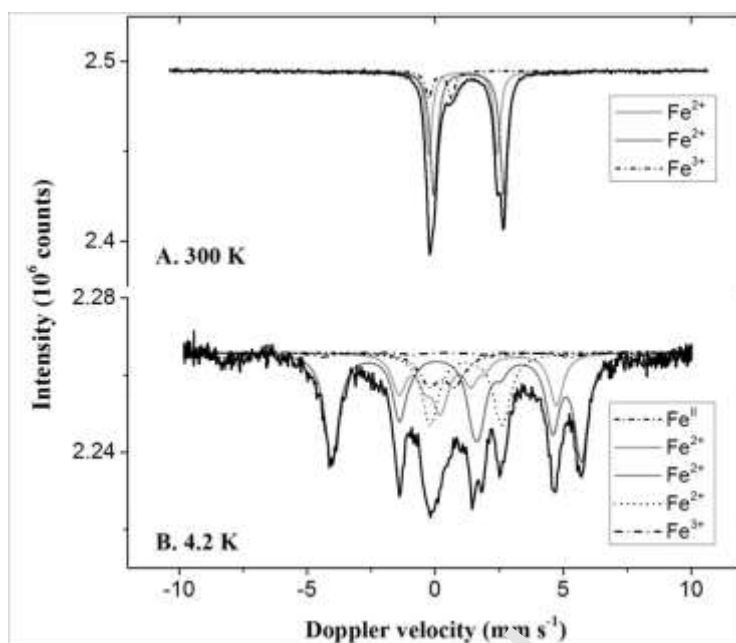


Figure A. 13: Mössbauer spectra obtained at different temperatures with A-stage sludge solids sampled in Nieuwveer.

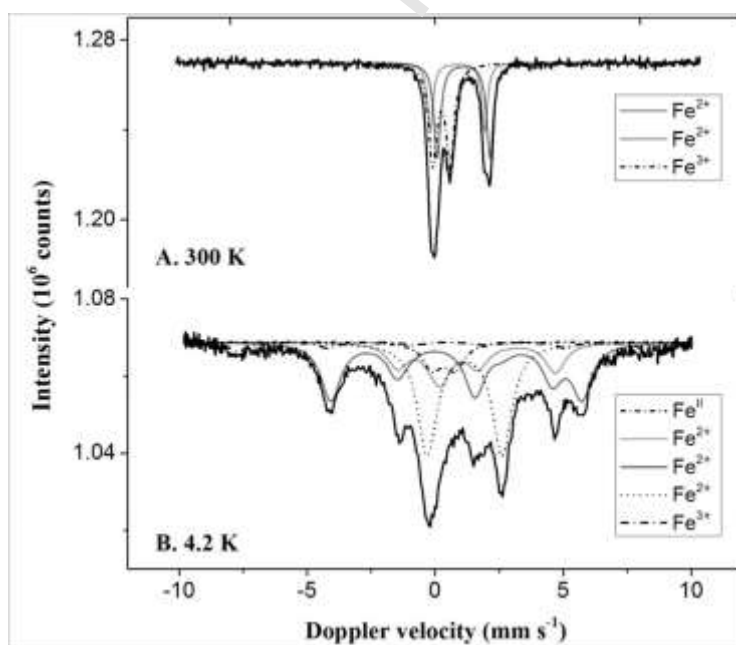


Figure A. 14: Mössbauer spectra obtained at different temperatures with B-stage sludge solids sampled in Nieuwveer.

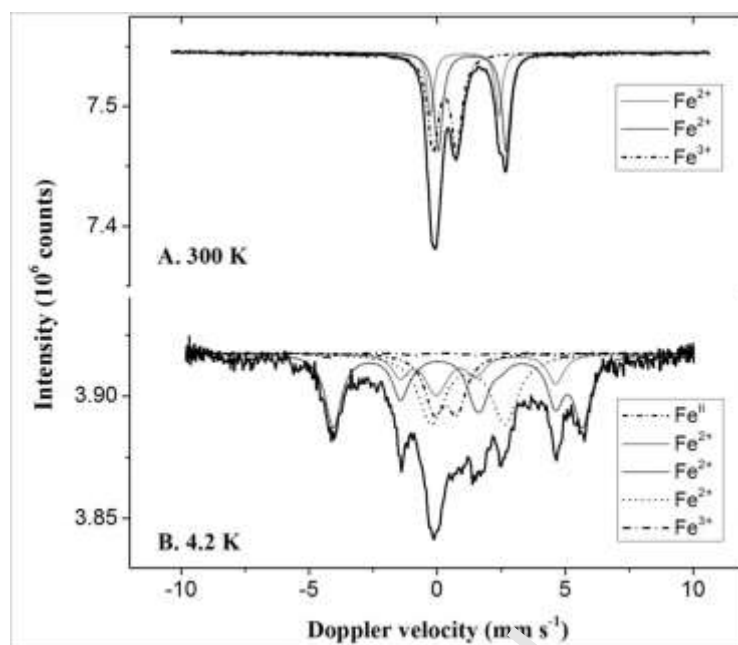


Figure A. 15: Mössbauer spectra obtained at different temperatures with digested sludge solids sampled in Nieuwveer.

Highlights:

- Fe chemistry and its correlation with P in two sewage treatment plants (STPs) was studied
- Surplus and digested sludge solids in the investigated STPs were dominated by Fe(II)
- The Fe(II)P mineral vivianite was a major iron compound in all samples
- We hypothesize: Vivianite is a key compound in all STPs and offers new P recovery routes